Antimicrobial potential of *C.sativum* seed extract against *S.aureus* In vitro, ADMET, Dockingand MD simulation

Sharmil Suganya R[1], Sugan.S[2], Venugopal T[3*],

[1*]Assistant Professor (Bio Engg), Government College of Engineering, Salem-11, Tamil Nadu, India

[2]Research Scholar (Chemistry), Government College of Engineering, Salem-11, Tamil Nadu, India

[3*]Assistant Professor (Chemistry), Government College of Engineering, Salem-11, Tamil Nadu, India

*Corresponding authors - venupaper@gmail.com, sweetsharmil@gmail.com

Orcid ID - https://orcid.org/0000-0003-2806-0139

https://orcid.org/0000-0001-7623-9518

Abstract

In this study, seeds of *C.sativum* purchased from market were extracted using Soxhlet extraction in vitro from which 38 active components were confirmed by GC – MS and FT – IR analysis. All the 38 ligands were docked using Autodoc vina with the four proteins (PDB ID: 4F6X, 3ACX, 2ZCQ, 2ZCS) obtained from RCSB PDB. Out of 38, two ligands from plant extract (2, 4-DTBP and 3-ethyl-5-isopropyl-2-methyl phenol) showed good docking scores of more than -7.5 Kcal / mol. Among those four proteins, PDB ID 4F6X has highest docking affinity of -.7.9 Kcal / mol than the other compounds. Well diffusion method confirmed the anti -microbial activity. In silico analysis using ADMET studies showed that the compounds have high log Kp value, high GI, BBB permeability, high HIA and low toxicity levels. Non violation of Lipinski's rule of five was found in both the ligands. Also, the values of Hydrogen Bond, RMSD, RMSF, SASA and Rg falls within a good range. In post MD, MM – PBSA studies, the results showed that the total binding free energies are more contributing in 3ACX and 2ZCS complexes than in 4F6X and 2ZCQ complexes. Hence, both the in vitro and in silico studies provide the evidence that the two active components have good interaction with the four protein targets.

Keywords

Docking, Molecular Simulation, RMSD, RMSF, SASA, Radius of Gyration

Abbreviation

ADMET - Absorption Distribution Metabolism Excretion, Toxicity, C.sativum – Coriandrum sativum, ARG – Arginine ASP – Asparate, ASN - Asparagine, BBB – Blood Brain Barrier, DS - Dock Score, DS 3.0 - Discovery Studio 3.0, 2, 4-DTPB - 2, 4-di-tert-butyl phenol, Electrostatic energy - $\Delta E_{Electro}$, Entropy - ΔS, FTIR – Fourier Transform and Infrared, GC-MS - Gas Chromatography - Mass Spectroscopic, GI – Gastrointestinal absorption, GLN – Glutamine, GLY – Glycine, HBA – Hydrogen Bond Acceptor, HBD – Hydrogen Bond donor, HIA – Human Intestinal Absorption, HIS – Histidine, Octanol - water partition coefficient – log P, Oral rat Acute toxicity – LD50, Non polar solvation energy- ΔG_{np}, Molecular Mechanics Poisson- Boltzmann Surface Area - MMPBSA, PDB – Protein Data bank, Polar solvation energy - ΔG_{solv}, Polar solvation free energy - ΔG_{polar}, RCSB - Research Collaboration for Structural Bioinformatics, Rg - Radius of gyration, RMSD - Root-Mean Square Deviation, RMSF - Root- Mean Square Fluctuation, SASA - Solvent-Accessible Surface Area, S.aureus – Staphylococcus aureus, Total Binding energy - ΔG_{bind}, TPSA – Total Polar surface area, TYR - Tyrosine, Vander Waal's energy - $\Delta EVDW$

1. Introduction

C. sativum is a herbal plant, of family *Apiceae* and genus of *Coriandrum*, is highly noted for its medicinal uses [1]. The anti-microbial activity of its leaves is one of the most reported biological activities [2, 3, 4]. They showed inhibitory activity against Gram-positive bacteria (e.g. *S. aureus* and *Bacillus* spp) and Gram-negative (e.g. *E. coli, P. aeruginosa, S. typhi, K. pneumoniae and P. mirabilis*. The phytochemical screening of *C. sativum* showed that itcontained essential oil, tannins, terpenoids, reducing sugars, alkaloids, phenolics, flavonoids, fatty acids, sterols and glycosides [5]. The taxonomic profile Kingdom of *C. sativum* is as follows: Plantae Subkingdom: Tracheobionta; Superdivision: Spermatophyta; Division: Magnoliophyta; Class: Magnoliopsida; Subclass: Rosidae; Order: Apiales; Family: Apiaceae; Genus: Coriandrum L.; Species: Coriandrum sativum L [6, 7]. 2,4-DTBP commonly occurs in the violate or essential oils of many seed plant species [8]. *S. aureus* is a Gram-positive bacteria, which causes severe toxin-mediated and invasive disorders including urinary tract infection, skin and soft tissue infections, pulmonoray infections, bacteremia, septic arthritis, meningitis, osteomyelitis, gastroenteritis and toxic-shock syndrome. The proteins of organisms can be taken from RCSB PDB. Thereby, four proteins were chosen : PDB ID: 4F6X is a Crystal structure of dehydrosqualene synthase (crtm) from s. aureus complexed with bph-1112. ([9], RCSB PDB). PDB ID: 3ACX is a Crystal structure of the C(30) carotenoid dehydrosqualene synthase from Staphylococcus aureus complexed with BPH-673 (Fu yang et al 2010, RCSB PDB). PDB ID: 2ZCQ is a Crystal structure of the C(30) carotenoid dehydrosqualene synthase from Staphylococcus aureus complexed with bisphosphonate BPH-652

([10], RCSB PDB). PDB ID: 2ZCS is a Crystal structure of the C(30) carotenoid dehydrosqualene synthase from Staphylococcus aureus complexed with bisphosphonate BPH-700 ([10], RCSB PDB).

2. Materials and Methods

2.1 Preparation of plant extract from C.sativum seed (ligands)

The seeds of the *C.sativum* were purchased from the market and was extracted in ethanol by Soxhlet extraction in vitro. Thereby, 38 active components were confirmed by FT-IR and GC-MS analysis. Canonical smiles were drawn using Chem draw tool for further investigations. They are given in detail as follows:

2.2 Soxhlet extraction

A Soxhlet extraction system is preferable for the continuous extraction of a solid with a hot solvent. About 50 g of dry powder were removed and used to create a porous thimble using a strong filter paper, which was then stored in the Soxhlet device. The seed material was extracted using one liter of ethanol. Boiling chips were added to the flask with a circular bottom and the device was set up for approximately 48 hours. The solvent was gradually brought to a boil; the vapor went through the tube, condensed in the condenser, and then filled the Soxhlet's body with the condensed solvent. The thimble's bottom was filled with a wool plug. The ratio of solute to solvent remained constant at 1:10. The solvent was poured into the RB flask after it reached the top of the tube, removing the portion of the material that had been extracted from the porous thimble. Up till the extraction was finished, the procedure was repeatedly carried out. This process took 48 hours in total, and the conclusion was that the colors of dark green, green, and yellow gradually changed to pale yellow, then to colorless. The gradual fading of color from dark green to colorless suggests a stepwise depletion of various pigments and organic compounds, reflecting the efficiency and completeness of the Soxhlet extraction process over time. Initially, the solvent dissolves highly concentrated colored compounds such as dark green. As the extraction continues, pigments with lower solubility or different chemical properties (such as carotenoids, which are yellow) dissolve into the solvent. The gradual fading of color to pale yellow suggests that the more soluble green compounds were extracted first, leaving behind less intense yellow pigments. Following extraction, the filtrate was dried using a rotary evaporator set to 55 degrees Celsius to produce a crude ethanol extract. Following that, a number of preliminary phytochemical analyses were conducted on the plant extracts that included secondary metabolites.

2.3 Well Diffusion Method

Using the Gram-positive (S. aureus) bacteria, the plant extract's antibacterial activity was

assessed. The bacterial strain was incubated at 37º C in LB broth. Using a spectrophotometer, the bacterial growth was harvested using 5 milliliters of sterile saline water. Its absorbance was measured at 580 nm, and it was diluted to achieve a viable cell count of 107 CFU/mL. To assess the plant extract's antibacterial properties, the well diffusion method was employed. After dissolving the ethanol extract in 10 mL of DMSO solvent, a Millipore filter (0. 22 mm) was used to sterilize the material. In sterile petri dishes, 10 mL of LB agar medium was sterilised and let to stand for 15 minutes. Using a sterile L rod, 100 µL of the bacterial slurry was distributed among the corresponding plates. Using a sterile cork borer, 8 mm diameter wells were created in the agar medium. The plant extract was then added to the wells at three different doses (10, 30 and 50 µL), along with positive and negative controls (50 µL each). The same was made into three duplicates. The plates were incubated for twenty-four hours at 37º C. After incubation, the zone of inhibition was measured and recorded using a vernier caliper. Therefore, the minimal inhibitory concentration of plant extract was assessed using the well diffusion method.

2.4 Gas Chromatography – Mass Spectroscopic (GC-MS) Analysis

In gas chromatography, a sample is injected and evaporated onto the tip of the chromatographic column utilizing Perkin Elmer Clarus SQ8C, specifically in gas-liquid chromatography. The gaseous mobile phase flow moves the sample through the column. A specific temperature is used for the elution of the analyses. Mass spectrometry is used to analyze the eluted analyses, which are then coupled with the built-in library. Microbial extracts and the plant environment can be analyzed to find undiscovered chemicals.

2.5 Fourier Transform - Infra Red (FT-IR) Spectroscopic Analysis

It is an analytical method for determining the composition of polymeric, organic, and occasionally inorganic materials. Manufacturer: Perkin Elmer Model: Spectrum Two Range: 400 cm-1 to 4000 cm-1 at a 4 cm-1 resolution Procedure: KBr pellet Samples: liquids and solids. Using this method, the frequency absorptions of the infrared radiation absorbed by the sample material are measured. The structure and vibration of molecular bands are identified via the infrared absorption bands.

2.6 Preparation of protein targets

From protein Data Bank (PDB) four protein structures of *S.aureus* (PDB ID: 4F6X, 3ACX, 2ZCQ, 2ZCS) were acquired via RCSB (www.rcsb.org).

2.7 ADMET, pharmacokinetic studies, Docking and MD simulations

Using Chemdraw 20.1.1, the ligand structures and smiles were drawn for the ligands.

Hydrogens are build and added using Avogadro tool. The drug-likeness, ADME, and toxicity of the molecule were assessed using online resources created by SwissADME (http://www.swissadme.ch/), Pro Tox 3.0 (https://tox.charite.de/protox3/), admeSAR (http://lmmd.ecust.edu.cn/admetsar2/), and Pre ADMET (https://preadmet.webservice.bmdrc.org/). Determining the drug-likeness attribute has proven to be especially useful in drug development studies since it can reduce the number of hitcompounds to consider for in vivo and in vitro research (Lipinski et al 2004). This helps us to predict ADME parameters, pharmacokinetic properties, drug like nature and medicinal chemistryfriendliness of one or multiple small molecules to support drug discovery [11]. The four protein targets of *S.aureus* were obtained from RCSB PDB (www.rcsb.org) and water molecules were removed by using BIOVIA Discovery Studio (Discovery Studio 2020). Using autodock tools, the pdb files were converted into pdbqt, and the ligand was made by following the steps below. Gaussian software was used to optimize the ligand before autodock tools were used to convert it to pdbqt.

2.8 Molecular Dynamics

An excellent method for studying atomic-level data regarding ligand binding to target molecules (proteins, DNA, or RNA) is through MD simulation [12, 13]. MD simulations of small-molecule inhibitors with their target proteins provide insights into the system's flexibility and stability, and the reliability of the binding mode [14]. Studies of molecular dynamics are helpful in figuring out conformationalchanges, hydrogen bonding interactions, and protein ligand complex stability [15]. The complex's stability suggests that the ligand can attach to the protein and alter its structural makeup. Gromacs 2020 was utilized in this work to analyze the molecular dynamics. The GROMACS software's Charms force field was employed for finding the interaction energy between the protein and TBNP for the 100 ns MD simulation. The temperature and pressure of the simulation was set at 300 K and 1 bar. The protein and ligand gro files were combined to create the topology for the protein-ligand complex. Ligand topology was constructed using the Swissparam website (http://www.swissparam.ch/). In this work, a simple point charge water (spc216) model and a dodecahedron box with a size of 1 nm were employed. GROMACS software tool was used to measure H bond, SASA, RMSD, RMSF and Radius of Gyration. GMX-MMPBSA was used for the molecular mechanics Poisson-Boltzmann surface analysis (MMPBSA) to determine the binding free energy and free energy changes [16].

3. Results and Discussion

4.1 Gas Choromatogrphy - Mass Spectroscopic analysis

From the Figure 1, it was concluded that though there were presence of phytoactive

compounds such as 1-methyl-3-(1-methylethyl), ç-terpinene, propane, 2-methyl, (2- mercaptoethyl) guanidine, 1,1,3-triethoxy in *C. sativum,* 2,4-Di-tert-butylphenol at retention time 11.562 with area % of 0.132, 3-ethyl-5-isopropyl-2-methyl phenol at retention time 8.416 with area % of 0.767 were chosen as best ligands as they gave good docking score in Autodoc vina. The table 1 shows the retention time and area % of the 38 active components present inthe plant extract by GC – MS [17, 18].

4.2 Fourier Transform - Infra Red spectroscopic analysis

In the present investigation, Figure 2 shows the FT - IR spectra of *C. sativum.* The peaks at cm^{-1} and the possible functional groups present in *C. sativum* were examined and given in the Table 2. From the Figure 2, it was evident that C=C, C-H, O-H, C=O, C-O stretching were possible due to the adsorption of these functional groups present in the active components of the plant extract. Table 2 shows the possible functional groups present in the plant extract.

From the Table 2, it was evident that the possible functional groups observed at different peaks were O-H, C=O, C-O in *C.sativum*. This showed that generally, the plant extracts used in this study might contain mixtures of compounds, i.e., alkaloids, flavonoids and organic acids. Table 3 represents the canonical smiles and structures drawn (using Chemdraw tool) for the 38 ligands extracted from *C.sativum.*

4.3 Minimum inhibitory concentration (well diffusion method)

In the present investigation, the well diffusion method was used as the primary or testing method to check whether the plant extract was able to inhibit the microbe on the plates. The plant inhibitor such as *C. sativum* consisting of different concentrations viz., T1, T2, T3 (10, 30 and 50µL respectively), a Negative - N (Di - methyl sulfoxide - DMSO) and a Positive - P (amoxyllin) controls of 50 µL each were shown in the Figure 3.

As the well diffusion, method showed clear zone of inhibition, the minimum inhibitory concentration was evaluated using well diffusion method as shown in Tables 4. The minimum inhibitory concentration of 30 ppm of *C. sativum* showed 12 mm zone of inhibition in *S. aureus*. This study revealed that the minimal inhibitory concentration for the plant extract to inhibit the growth of *S. aureus* was found to be 30 ppm. In this study, the plant extract inhibited the bacterial growth on the plates. Negative - N control, Positive - P control, T1 10 µL, T2 30 µL , T3 50 µL shows 10, 13, 11, 12, 13 mm respectively. From the clear zone of inhibition, i.e., on an average of around 12 mm, 30 ppm of the inhibitor was identified as a sufficient dosage showing good antimicrobial activity.

4.4 Molecular Docking Studies of the Extract

All the 38 active components (ligands) of plant extract were docked with *S.aureus* four proteins using Autodoc vina [19, 20] to find the highest docking score. Table 4 gives the docking scores (Kcal / mol) obtained for 38 active components of *C.sativum* with *S.aureus* four proteins using Autodock vina tool. The docking scores seem to be less for all other ligands when compared to 2,4-Di-tert-butylphenol and 3-ethyl-5-isopropyl-2-methyl phenol. Thereby, these two active components were considered as best ligands: ligand 1 and ligand 2 respectively for further docking studies.

Fig 4a shows the protein-ligand docking of ligand 1 with 4F6X having conventional H bond with a distanceof 2.78894 Å. Fig 4b shows the protein-ligand docking of ligand 2 with 3ACX having conventional H bond with a distances of 3.0404, 2.38693, 2.6893, 3.08172, 2.7766 (Å). Fig 5a shows the protein-ligand docking of ligand 2 with 2zcq having conventional H bond with a distances of 3.15161, 2.30173 (Å). Fig 5b shows the protein-ligand docking of ligand 1 with 2ZCS having conventional H bond with a distances of 2.54168, 2.3792, 2.41426, 3.02218 (Å).

The table 5 represents the results of Molecular Docking. Initially, the ligands, 2,4-Di-tert-butylphenol and 3-ethyl-5-isopropyl-2-methyl phenol were targeted against PDB ID: 4F6X, to decipher the molecular interactions. In this, ligand 1 had good interaction with polar HIS18 (N-H…O) (2.788 A°) (Dock score -7.9 Kcal/mol) which showed one hydrogen bond interaction. Similarly, the ligands were targeted against PDB ID: 3ACX., but, ligand 2 only interacted well with polar GLY138 (N-H…O) (3.040 A°), ASN168 (O…H-N) (2.386A°), ASN168 (O…H-N) (2.678 A°), ARG45 (N-H…N) (3.081 A°), TYR41 (N-H…O) (2.776 A°) (Dock score -7.7 Kcal/mol) which showed five hydrogen bond interactions. When the ligands were targeted against PDB ID: 2ZCQ, ligand 2 interacted well with polar GLY138 (N-H…O) (3.151 A°) and GLY161 (N-H…O) (2.301 A°) (Dock score -7.7 Kcal/mol) which showed two hydrogen bond interactions. With PDB ID: 2ZCS, ligand 1 interacted well with polar GLN165 (N-H…N) (2.541A°), ASP49 (O…H-N) (2.379 A°), ASN168 (O…H-N) (2.414 A°), TYR41 (N-H…O) (3.022 A°) (Dock score -7.5 Kcal/mol) which showed four hydrogen bond interactions. Form the above, it is found that the ligand 1 with PDB ID : 4F6X reported highest affinity (-7.9 Kcal / mol) when compared to all the others (Table 5). Effective hydrogen bonding distinguishes distinct functional groups that might be in charge of further hydrogen bonding, producing an effect of these compounds with high binding affinities against target proteins, which could be crucial in resistance to infection [21].

4.5 Drug Likeliness, ADMET, Pharmacokinetic parameters and Toxicity prediction by SwissADME and Protox II tools

Table 6 represents the ADMET, Pharmacokinetics and Drug likeliness properties predicted by SwissADME and ProTox II tool. Before conducting in vitro, in vivo, or preclinical investigations, it is necessary to evaluate the initial empirical understanding of the physiochemical properties of lead compounds. In this study, as per the predictions, the two compounds did not violate Lipinski's rule, Ghose, Veber and Egan [22, 23]. But there is violation of Mugge in both. In both the compounds,the Gastrointestinal absorption was found to be high. The Total polar surface area (TPSA) is 20.23 $Å^2$ respectively. Both have one Hydrogen Bond acceptor (HBA) and one Hydrogen Bond donor (HBD) each. Log P is less than 5 in both, so, it is good for oral and intestinal absorption. As both the compounds does not violate the Lipinski's rule of five, it can be used as orally activedrug in Human beings. The lethal doses of the substance LD50 shall be given are 700 mg / kg, 1030 mm/kg respectively.

The CaCo2 permeability of the two compounds were found to be 0.8168 cm/s, 0.8560 cm/s, respectively. The two compounds reported high logarithm of the permeability coefficient log Kp values in cm/s (-4.68 and -4.65), indicating minimal skin penetration. Studies have shownthat chemical compounds with a log Kp value greater than -2.5 can't get through the skin very well. This is because the metabolites are more easily dissolved. The results show that thecompounds can be easily absorbed by the body and the molecule can be transported through different parts of the body. Blood Brain Barrier is also high in both the compounds.

If the HIA is between 70 and 100%, it signifies outstanding gastrointestinal absorption. Conversely, if the HIA is below 30%, it suggests insufficient absorption. The two compounds with confirmed HIA values of 99.52% and 99.66% exhibit elevated levels of absorption. P-glycoprotein (Pgp) has a crucial function in drug metabolism, influenced by both the inhibition and induction of therapeutic medicines. CYP models, based on either the substrate or inhibitor, analyse the process of drug metabolism. The significant target such as CYP2C19 substrate, CYP2C9 substrate, CYP3A4 substrate (2, 4-di-tert-butyl phenol) and (3- ethyl-5-isopropyl-2-methyl phenol) were found to be non-inhibitor (the drugs in the bracket did not inhibit the target), they acted as inducers. The results shows that the two compounds havelow levels of toxicity levels for T. pyriformis, as indicated by their minimal acute oral toxicity values.

4.6 Molecular Dynamics Trajectory analysis

MD simulation studies were carried out to investigate their binding affinity and stability in the ligands' active sites. This simulation was carried out in four stages as Minimization, Heating, Equilibration and Production by using CHARMM force field. To analyze and gain insight into the structural stabilities, binding modes, and binding strengths of the proposed molecules, the complexes' SASA, RMSD, RMSF, Rg were computed using Gromacs software.

Figures 6a-1, 6a-2, 6b-1, 6b-2 depicts the Hydrogen bond variation during MD simulation of protein - ligand complex. The increased stability of the complex during the simulation was due to the higher number of conventional bonds. The PDB ID 2ZCS showed the Highest variation with 4 hydrogen bonds. Others showed a maximum of two hydrogen bonds. In particular, 2ZCQ and 3ACX complexes showed no hydrogen bonds for a period of simulation and then showed two hydrogen bonds.

To assess the stability of the protein and ligand–protein complexes, a root-mean-square deviation (RMSD) analysis [24] was conducted on Gromacs, as shown in Figure 7a-1, 7a-2,7b-1, 7b-2 and Table 3. Previous reports showed that Good RMSD values falls ≤ 2.0 Å and bad (RMSD ≥ 3.0 Å). Thereby, the ligand fits efficiently into the pocket (target protein). The ligand properly orients and interacts strongly with the protein.

In this study, 4F6X and 2ZCS complexes are in 3.0 Å, hence structurally not stable. The 3ACX and 2ZCQ complexes are less than 2.0 Å, hence structurally stable. Whereas, the proteins in all the four plots are less than 2.0 Å, hence stable. Therefore, it can be concluded that the stability of ligand-protein complexes 3ACX and 2ZCQ are good and structurally stable.

Fig 8a-1, 8a-2, 8b-1, 8b-2 shows the proteins Root mean square Fluctuations (RMSF) in complex withthe ligand during 100 ns in MD simulations. Lower the variation in RMSF, lower the values will be, more the protein ligand complex stable [25]. The values of RMSF shows the fluctuations in amino acids. It is used to check the flexibility of residues within a protein during the course of the simulation. In all the four plots, all the proteins and the protein – ligand complexes showed approximately 0.15 Å which is very low. The fluctuations in aminoacids seems to be same in all the four proteins, protein - ligand complexes. This low RMSF represents low flexibility of protein without ligand. Hence no conformational changes and structurally stable.

Studies on the radius of gyration (Rg) are useful in comprehending how the tertiary structure of protein-ligand complexes changes [26]. A lower Rg value suggests that the protein undergoes less conformational change, more stability and that the tertiary structure is unaffected. Both the Rg plots of 4F6X, 3ACX show interaction with the protein and the ligand, but still they are below 2 nm, thereby no alteration in the tertiary structure. Both the proteins 2ZCQ, 2ZCS plots seems to be similar and shows Rg to be within 2 nm, and their complexes are below 0.2 nm, indicating that neither protein nor the complex alters the tertiary structure (Fig 9a-1, 9a-2, 9b-1, 9b-2).

Solvent accessible surface area (SASA) analysis shows the protein-ligand complex with solvent with respect to time. The average values for PDB ID 4F6X, 3ACX, 2ZCQ, 2ZCS ligand

complex were 150, 153, 151, 152 nm^2, respectively. In all the four plots, SASA value is low, out of which, 4F6X complex shows lowest SASA value during MD simulation of 100 ns whereas, the other protein – ligand complexes showed a little higher values than 4F6X. There is no protein structure expansion as the SASA values are found to be less in all the four plots which means the complex structures are stable (Fig 10a-1, 10a-2, 10b-1, 10b-2).

4. 7 Post MD simulation MM-PBSA

After MD, the free binding energy of the ligands were calculated using the MM - PBSA method from the trajectories of the Protein–ligand complexes to further confirm the results. This strategy has been extensively used as a dependable and effective free energy modeling technique to simulate molecular recognition, including interactions between proteins and ligands. Many researchers used enriched datasets containing known active molecules along with decoys to evaluate the MM/PB(GB)SA approach's reliability for virtual screening studies [27, 28]. They then compared the approach's predictive power to other approaches, specifically to the docking programs' scoring functions [29]. MM / PB (GB) SA have already been extensively used for predicting these interactions : Protein- protein interactions, including those involving proteins and peptides, protein-DNA interactions, and protein-RNA interactions, which in turn can be highly helpful in the study of molecular mechanics and the development of novel active ligands [30]. The energy contribution of the various energetic terms (van der Waals energy, electrostatic energy, polar solvation energy, and non-polar solvation energy/SASA) to the total binding energy are given in table 7. The results refer to averages over last 1000 frames. The energy values are given inkJ/mol [31]. We also ascertain the individual contributions to the bindingfree energy in order to clarify the binding mechanisms. This time, the vander waal's contribution between the proteins and the ligands, electrostatic interactions, represented by ΔE_{elec} or ΔE_{vdW}, the polar or nonpolar solvation free energy, represented by ΔG_{polar} or ΔG_{np}, ΔG_{solv}, represented by Polar solvation energy, SASA energy / non polar solvation energy and the contribution from the binding partners' configurational entropy, indicated by ΔS, ΔG_{bind} (Total Binding Energy) were all taken into account [32]. The Vander waals term is unfavourable in 4F6Xand 2ZCS complexes and contributes least to the binding energy. Whereas, the electrostatic energy in 3ACX complex is unfavorable and contributes least to the binding energy. [33]. There is no SASA energy in 4F6X and 2ZCQ complexes. The total binding free energies are found to be -14.02 to -16.1 in 3ACX and 2ZCS complexes. The non polar interaction with the solvent, ΔG_{np} values are contributing to the binding energy in all the four complexes and ranges from -24.23 to -2383.65 kCal / mol. Association is opposed by anunfavorable desolvation of polar groups, ΔG_{polar}, yielding a contribution of 7.28 to 2390.63 kcal/mol for all protein – ligand complexes.

A reduction in the configurational entropy of the binding partners is often antagonistic to the formation of macromolecular complexes [34]. When a tiny molecule binds to a protein, its mobility is restricted, which results in a loss of configurational entropy and a decrease in binding affinity [35, 36]. The corresponding loss in entropy due to the translational, rotational, and vibrational degrees of freedom made free energy contributions between 2.23 and 84.15 kcal/mol for all protein−ligand complexes. Since the contribution of the ΔS is more favourable to the complexes of 3ACX and 2ZCS than 4F6X and 2ZCQ and the SASA energy is found to be zero for 4F6X and 2ZCQ, but more favourable for 3ACX and 2ZCS, it is concluded that total binding free energies are more contributing in 3ACX and 2ZCS complexes.

4.8 Radial Distribution Function g(r)

From the figures 11 and 12, on comparing the complexes of 4F6X & 2ZCQ, both display a broad region of close to zero spike, and then it dampens to $g(r)\approx1$, exhibits an absence of structural correlation past a moderate excluded distance and Indicates greater disordering or a more uniform distribution of these atoms/molecules in the sample. On comparing the complexes of 3ACX & 2ZCS, they display evident short and medium range ordering with numerous identifiable peaks. Particularly 2ZCS has very strong peak intensities which suggest very strong or repetitive local correlations. All of them finally attenuate to 1 for large r as expected for a fluid or amorphous medium with no pronounced long range order.

5. Conclusion

The seeds of *C.sativum* were extracted in ethanol by Soxhlet extraction method and 38 active components were found from the extract by the GC – MS analysis and FTIR analysis. Then, 4 target proteins (PDB ID: 4F6X, 3ACX, 2ZCQ, 2ZCS) of *Staphylococcus aureus* were chosen from RCSB PDB. All the 38 active components were taken as ligands and docked with the 4 target proteins using Autodoc vina. Out of those 38, only two active components (ligands), 2, 4-di-tert-butyl phenol and 3-ethyl-5-isopropyl-2-methyl phenol were found to have high docking scores more than -7.5 Kcal / mol. These two ligands have more inhibitory effect as it might have some phytochemicals like alkaloids, flavonoids, tannins, saponins, and terpenoids**.** The interaction of the plant extract with *S.aureus* was confirmed by the well diffusion method as the clear zones of inhibition were obtained confirming anti-microbial activity. In silico ADMET studies using SwssADME and ProTox II revealed that compounds can penetrate the body easily by their log Kp values of < 2.5,high BBB, about 99% elevated level s of HIA, low cytotoxicity. As the ligands did not violatethe Lipinski's rule of five they can be taken as oral drugs in Humans. The RMSD values of 4F6Xand 2ZCS complexes are in 3.0 Å, hence structurally not stable. The 3ACX and

2ZCQ complexes are less than 2.0 Å, hence structurally stable. The low RMSF values indicates that the flexibility of the proteins are low and so no conformational changes occurs, and hence, the protein – ligand complexes in all the four plots are structurally stable. The SASA values are found to be less in all the four plots which means that there is no protein structure expansion and hence, the complex structures are stable in all the four plots. The Rg plots of 4F6X, 3ACX show interaction with the protein and the ligand, but still they are below 2 nm, thereby no alteration in the tertiary structure. Both the proteins 2ZCQ, 2ZCS plots seems to be similar and shows Rg to be within 2 nm, and their complexes are below 0.2 nm, indicating that neither protein nor the complex alters the tertiary structure. In post MD, MM – PBSA studies, the results showed that asthe contribution of the ΔS is more favourable to the complexes of 3ACX and 2ZCS than 4F6X and 2ZCQ and the SASA energy is zero for 4F6X and 2ZCQ, but more favourable for 3ACX and2ZCS, therefore the total binding free energies are more contributing in 3ACX and 2ZCScomplexes. From the results of this study, it was concluded that the effect of the two ligands against the protein targets were feasible and reliable.

Acknowledgments

We would like to extend our heartfelt thanks to the Government College of Engineering, Salem, for giving us the chance to properly complete our research work. We extend our gratitude to the scientific staff members of the Department of Chemistry Laboratory for their invaluable assistance over the course of the experimental research.

Authors' contribution:

R. Sharmil Suganya: Planning and conduction of experiments, result analysis and manuscript writing; S,Sugan: Conduction of experiments; T. Venugopal: Planning and conduction of experiments, Editing the manuscript and manuscript writing.

Research content: The research content of manuscript is original and has not been published elsewhere.

Ethical approval: No animals or living plants and/or injured during the study in associated environs.

Conflict of interest: The authors declare that there is no conflict of interest.

Consent to publish: All authors agree to publish the paper in this esteemed journal.

References

1. Najla Gooda Sahib, Farooq Anwar, Anwarul-Hassan Gilani, *et al.*, "Coriander (Coriandrum sativum L.): a potential source of high-value components for functional foods & nutraceuticals-a review", *Phytotherapy research Phytother. Res.* Published online in Wiley Online Library (wileyonlinelibrary.com), (2012), DOI: 10.1002/ptr.4897.

2. Kubo, I., Fujita, KI., Kubo, A., *et al*., "Antibacterial activity of coriander volatile compounds against salmonella cholerasuis", J Agri Food Chem, 52, pp. 3329- 3332, (2004), DOI: 10.1021/jf0354186.
3. Saeed, S., & Tariq, P., "Antimicrobial activities of emblica officinalis & coriandrum sativum against gram-positive bacteria & candida albicans", *Pak J Bot*, **39**, pp. 913-917, (2007), https://www.cabidigitallibrary.org/doi/full/10.5555/20073235231.
4. Begnami, A., F., Duarte, MCT *et al*., "Antimicrobial potential of coriandrum sativum l. against different candida species in vitro", *Food Chem*, **118**, pp. 74-77, (2010), https://doi.org/10.1016/J.FOODCHEM.2009.04.089.
5. Ali Esmail Al-Snafi, "A review on chemical constituents & pharmacological activities of coriandrum sativum", *IOSR Journal Of Pharmacy*, **6** (7), Version. 3, pp. 17-42 (2016) www.iosrphr.org (e)-ISSN: 2250-3013, (p)-ISSN: 2319-4219, https://www.iosrphr.org/papers/v6i7V3/D067031742.pdf, http://dx.doi.org/10.9790/3013-067031742.
6. Samba Murty, AVSS., & Subrahmanyam, NS., "A textbook of economic botany", *Wiley Eastern Limited, New Delhi*, pp. 416-419. (1989),
7. The plant list, "A working list of all plant species, coriandrum sativum", (2013), http://www.theplantlist.org/tpl1.1/record/kew-2737546.
8. Fuqiang Zhao, Ping Wang, Rima, D., *et al.*, "Natural sources and bioactivities of 2,4-di-tert-butylphenol and its analogs", *Toxins* **12**, 35, (2020) doi:10.3390/toxins1201003.
9. Yonghui Zhang, Fu-Yang Lin, Kai Li, *et al.*, "HIV-1 integrase inhibitor-inspired antibacterials targeting isoprenoid biosynthesis", *ACS medicinal chemistry letter*, ACS publications, *American Chemical Society*, ACS Med. Chem. Lett., **3**, pp. 402−406, (2012), dx.doi.org/10.1021/ml300038t.
10. Chia-I Liu, George, Y., Liu, *et al.*, "A cholesterol biosynthesis inhibitorblocks staphylococcus aureus virulence", *SCIENCE*, **319**, (2008), www.sciencemag.org, https://doi.org/10.1126/science.1153018.
11. Banerjee, P., Kemmler, E., Dunkel, M., *et al*., "ProTox 3.0: a webserver for the prediction of toxicity of chemicals", *Nucleic Acids Res* (Web server issue); NAR, (2024**),** https://doi.org/10.1093/nar/gkae303.
12. Hollingsworth, S., A., & Dror, R., O., "Molecular dynamics simulation for all", *Neuron*, **99**(6), pp. 1129–1143, (2018), https://doi.org/10.1016/j.neuron. 2018.08.011.
13. Kumari, P., Pratap Singh, S., & Som, A., "Insights into the dynamics of cyclicdiguanosine monophosphate I riboswitch using molecular dynamics simulation", *Indian Journal of*

Biochemistry and Biophysics (IJBB), **58** (3), 208–218, (2021), https://doi.org/10.56042/ijbb.v58i3.37679.

14. Tagyedeen, H., Shoaib, Nihal Abdelmoniem, Rua, M., *et al.*, "Molecular docking and molecular dynamics studies reveal the anticancer potential of medicinal-plant-derived lignans as mdm2-p53 interaction inhibitors", *Molecules*, **28**, pp. 6665, (2023), https://doi.org/10.3390/molecules28186665.
15. Deswal, Y., Asija, S., Aisha Tufail, Amit Dubey, *et al.*, "Instigating the in vitro antidiabetic activity of new tridentate schiff base ligand appended m(ii) complexes: from synthesis, structural characterization, quantum computational calculations to molecular docking, and molecular dynamics simulation studies", *Applied Organometallic Chemistry*, **37**(4), (2023), http://dx.doi.org/10.1002/aoc.7050.
16. Valdés-Tresanco, M., S., Valdés-Tresanco, M., E., Valiente, P., A., *et al.*, "gmx_mmpbsa: a new Tool to Perform End-State Free Energy Calculations with GROMACS", *Journal of Chemical Theory and Computation*, **17** (10), pp. 6281- 6291, (2021), https://pubs.acs.org/doi/10.1021/acs.jctc.1c00645.
17. Banerjee, P., Eckert, O., A., Schrey, A., *et al*., "ProTox-II: a webserver for the prediction of toxicity of chemicals", *Nucleic Acids Res* (Web server issue); NAR, (2018)
18. Keeling, CI & Bohlmann, J, "Genes, enzymes & chemicals of terpenoid diversity in the constitutive & induced defence of conifers against insects & pathogens", *New Phytologist*, **170**, pp. 657-675, (2006), https://doi.org/10.1111/j.1469-8137.2006.01716.x.
19. Phillips, M., A., Stewart, M., A., Woodling, D., L., *et al*., "Has molecular docking ever brought us a medicine", *Molecular Docking. London, UK: Intech Open*, 141–178, (2018), DOI: 10.5772/intechopen.72898.
20. Rott, O., and A., J., Olson, "AutoDock vina: improving the speed and accuracy of docking with a new scoring function, efficient optimization, and multithreading", *Journal of Computational Chemistry*, **31**(2): pp. 455-461, (2010), https://doi.org/10.1002/jcc.21334.
21. Abhishek Kumar Verma, Sk., Faisal Ahmed, Md., Shahadat Hossain, *et al.*, "Molecular docking and simulation studies of flavonoid compounds against pbp-2a of methicillin-resistant staphylococcus aureus", *Journal of Biomolecular Structure andDynamics*, **40** (21), (2022**)**, https://doi.org/10.1080/07391102.2021.1944911.
22. Lipinski, C., A., "Lead- and drug-like compounds: the rule-of-five revolution", *Drug Discov Today Technol*, **1**(4): pp. 337-41, (2004), https://doi.org/10.1016/j.ddtec.2004.11.007.
23. Lipinski CA., Lombardo F., Dominy BW., *et al*., "Experimental and computational approaches to estimate solubility and permeability in drug discovery and development settings". *Advanced*

Drug Delivery Reviews, **46** (1–3): 3, (2021), doi:10.1016/S0169-409X(00)00129-0. PMID 11259830.

24. Berishvili, V., P., Kuimov A., N., Voronkov, A., E., *et al.*, "Discovery of novel tankyrase inhibitors through molecular docking- based virtual screening and molecular dynamics simulation studies", *Molecules*, **25**(14), (2020), https://doi.org/10.3390/molecules25143171.
25. Lu Zeping, Yifei Zhang, Wei Zhang, *et al.*, "Lid and tunnel dynamics guided the modification of chitosan by ionic liquids for enhancing its immobilization performance of candida antarctica lipase b" *Journal of Molecular Liquids,* (2024), https://doi.org/10.1016/j.molliq.2024.125098.
26. Ismail, N., A., and Jusoh, S., A., "Molecular docking and molecular dynamics simulation studies to predict flavonoid binding on the surface of denv2 e protein", *Interdiscip Sci,* **9**(4): pp. 499-511, (2017), http://dx.doi.org/10.1007/s12539-016-0157-8.
27. Wang, E., Sun, H., Wang, J., "Free energy calculation with mm/pbsa and mm/gbsa: strategies and applications in drug design", *Chem Rev*. 119, pp. 9478–9508, (2019), https://doi.org/10.1021/acs.chemrev.9b00055.
28. Poli, G., Granchi, C., Rizzolio, F., "Application of mm-pbsa methods in virtual screening", *Molecules,* **25,** pp.1971, 2020, https://doi.org/10.3390/molecules25081971.
29. Tiziano Tuccinardi, "What is the current value of mm/pbsa and mm/ gbsa methods in drug discovery?", *Expert Opinion on Drug Discovery,* (2021) https://doi.org/10.1080/17460441.2021.1942836.
30. Lafont V., Schaefer M., Stote RH., "Protein-protein recognition and interaction hot spotsin an antigen-antibody complex: free energy decomposition identifies efficient amino acids.", *Proteins Struct Funct Bioinforma.,* **67**, pp. 418–434, (2007), https://doi.org/10.1002/prot.21259.
31. Vasanthanathan Poongavanam, Jo´gvan Magnus Haugaard Olsen and Jacob Kongsted, "Binding free energy based structural dynamics analysis of hiv-1 rt rnase h–inhibitor complexes", *Integrative Biology*, (2014), DOI: 10.1039/c4ib00111g www.rsc.org/ibiology.
32. Parimal Kar, Reinhard Lipowsky, and Volker Knecht, "Importance of polar solvation and configurational entropy for design of antiretroviral drugs targeting hiv-1 protease", *The Journal of Physical Chemistry,* American Chemical Society, dx., J. Phys. Chem. B, 117, 5793−5805 (2013), doi.org/10.1021/jp3085292.
33. Eberhardt, J., Santos – Martins, D., Tillack, A., F., *et al.*, "AutoDock vina 1.2.0: new docking methods, expanded force field, and python bindings" *Journal of Chemical Information and Modeling*, **61**(8): pp. 3891- 3898 (2021), https://doi.org/10.1021/acs.jcim.1c00203.
34. Fu-Yang Lina, Chia-I Liub,, Yi-Liang Liua, *et al.*, a Center for Biophysics and Computational

Biology, University, “Mechanism of action and inhibition of dehydrosqualene synthase”, *PNAS*, 107, 50, pp. (2010) 21337– 21342, https://doi.org/10.1073/pnas.1010907107.

35. Kijewska M., Sharfalddin A., A., Jaremko Ł., *et al.*, “Lossen rearrangement of p-toluenesulfonates of n-oxyimides in basic condition, theoretical study, and molecular docking”, *Front. Chem*., **9**, 662533, (2021), https://doi.org/10.3389/fchem.2021.662533.
36. Xu, Y., X., Liang, and Hyun, C., G., “Isolation, characterization, genome annotation, and evaluation of hyaluronidase inhibitory activity in secondary metabolites of brevibacillus sp. jnucc 41: a comprehensive analysis through molecular docking and molecular dynamics simulation”, *Int J Mol Sci*, **25**(9), (2024), https://doi.org/10.3390/ijms25094611.

Figure 1 GC - MS spectra of *C. sativum*

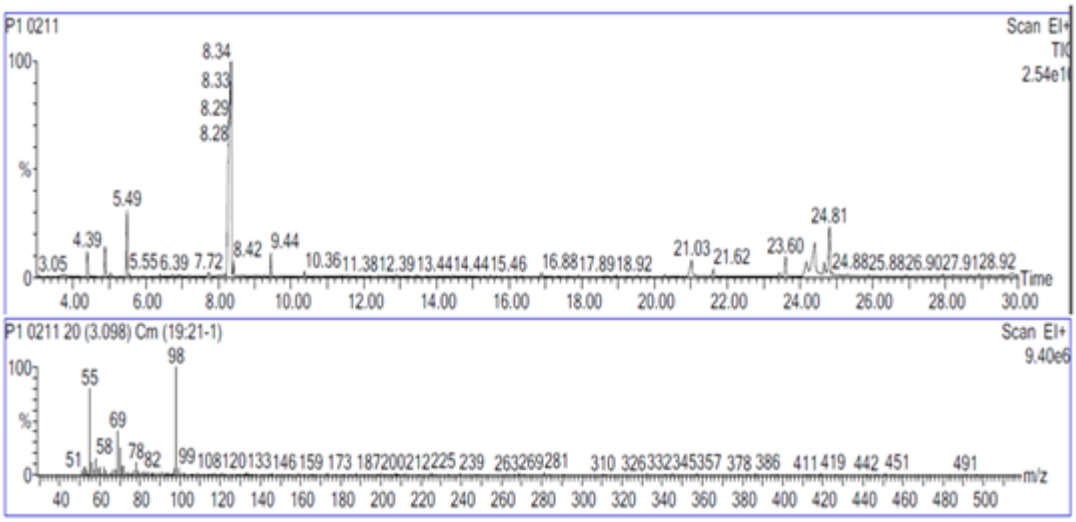

Table 1: Constituents of Inhibitor analysed by GC-MS

S.No.	Retention Time	Compound	Area %
1	3.098	Cyclopentanone, 2-methyl-	0.125
2	3.764	(2-Mercaptoethyl)guanidine	0.856
3	3.899	1,2-Diethylhydrazine	0.155
4	4.394	Benzene, 1-methyl-3-(1-methylethyl)-	2.766
5	4.884	ç-Terpinene	2.970
6	5.034	Propane, 1,1,3-triethoxy-	0.335
7	5.489	Linalool	5.767
8	5.549	Bicyclo[3.1.0]hexan-2-ol, 2-methyl-5-(1-methylethyl)-, (1à,2à,5à)-	0.188

9	6.745	Terpinen-4-ol	0.192
10	6.945	Terpineol	0.161
11	7.195	Bicyclo[3.1.0]hexan-2-ol, 2-methyl-5-(1-methylethyl)-, (1à,2à,5à)-	0.129
12	7.720	Thymoquinone	0.318
13	7.755	2-Cyclohexen-1-one, 2-(2-methyl-2-propenyl)-	0.391
14	8.030	Tenovin-6	0.139
15	8.135	Thymol	0.156
16	**8.416**	**3-ethyl-5-isopropyl-2-methyl phenol**	**0.767**
17	9.266	2-Methyl-5-(propan-2-ylidene)cyclohexane-1,4-diol	0.124
18	9.441	2,6-Octadien-1-ol, 3,7-dimethyl-, acetate	1.375
19	10.361	p-Cymene-2,5-diol	0.423
20	**11.562**	**2,4-Di-tert-butylphenol**	**0.132**
21	12.902	2-Tridecenal, (E)-	0.157
22	16.879	Tetradecanoic acid	0.416
23	19.520	Naphthalene, 1,2,3,4,4a,5,6,7-octahydro-4a-methyl-	0.143
24	20.275	Hexadecanoic acid, methyl ester	0.246
25	21.026	n-Hexadecanoic acid	3.677
26	21.616	Hexadecanoic acid, ethyl ester	0.727
27	23.437	9,12-Octadecadienoic acid (Z,Z)-, methyl ester	0.415
28	23.602	6-Octadecenoic acid, methyl ester, (Z)-	2.543
29	24.182	9,12-Octadecadienoic acid (Z,Z)-	3.124
30	24.407	9-Octadecenoic acid, (E)-	8.985
31	24.667	Linoleic acid ethyl ester	1.188
32	24.812	Ethyl Oleate	5.782
33	25.047	Butanedioic acid, 3-hydroxy-2,2-dimethyl-, diethylester	0.125
34	25.297	Octadecanoic acid, 17-methyl-, methyl ester	0.212
35	27.948	Methyl glycocholate, 3TMS derivative	0.204
36	28.224	Oxiraneoctanoic acid, 3-octyl-, cis-	0.241
37	28.924	Tricyclo[20.8.0.0(7,16)]triacontane, 1(22),7(16)-diepoxy-	0.151
38	29.834	Glycidyl oleate	0.378

Figure 2 FT - IR spectra of *C. sativum*

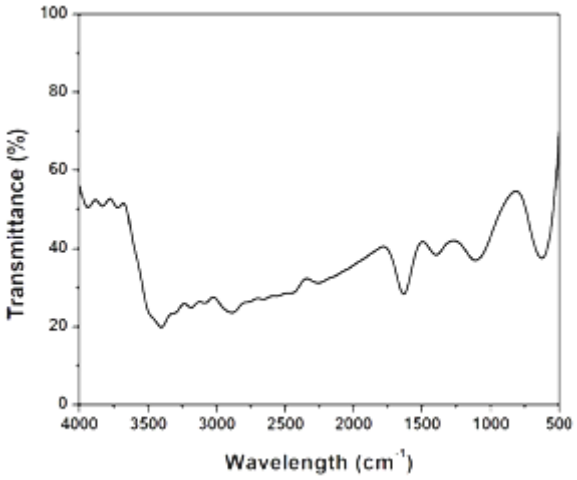

Table 2 Functional groups from FT - IR spectra of *C. sativum*

FTIR spectra of *C. sativum*	
Peaks at cm^{-1}	**Possible functional groups**
~3300	O-H
~1600	C=O
~1028	C-O

Table 3 Canonical smiles and Chem draw pictures of 38 ligands of *C.sativum*

S. No.	**Ligand name**	**Smiles from Chemdraw**	**Structures From Chemdraw**
1	Cyclopentanone, 2-methyl-	O=C1C(C)CCC1	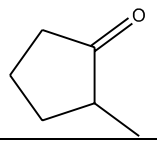
2	(2-Mercaptoethyl)guanidine	NC(NCCS)=N	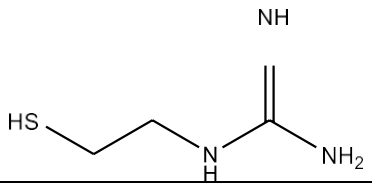
3	1,2-Diethylhydrazine	CCNNCC	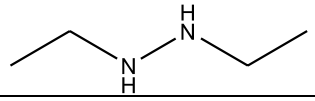

4	Benzene, 1-methyl-3-(1-methylethyl)-	CC(C1=CC(C)=CC=C1)C	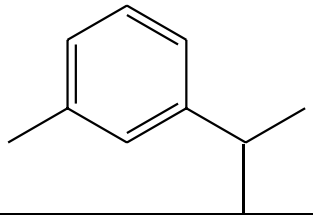
5	ç-Terpinene	CC(C)C1=CCC(C)=CC1	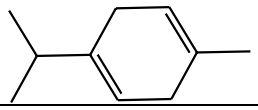
6	Propane, 1,1,3-triethoxy-	CCOCCC(OCC)OCC	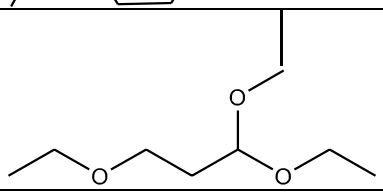
7	Linalool	C/C(C)=C\CCC(C)(O)C=C	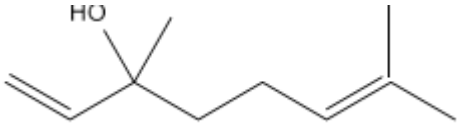
8	Bicyclo[3.1.0]hexan-2-ol, 2-methyl-5-(1-methylethyl)-, (1à,2à,5à)-	OC1(C)C2CC2(C(C)C)CC1	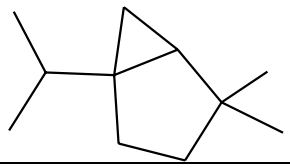
9	Terpinen-4-ol	CC1=CCC(C(C)C)(O)CC1	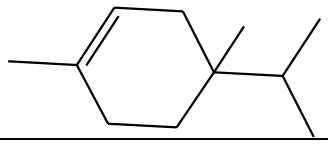
10	Terpineol	CC1=CCC(C(C)(O)C)CC1	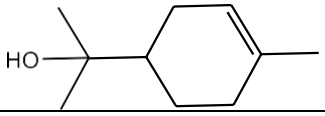
11	Bicyclo[3.1.0]hexan-2-ol, 2-methyl-5-(1-methylethyl)-, (1à,2à,5à)-	OC1(C)C2CC2(C(C)C)CC1	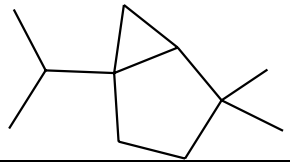
12	Thymoquinone	O=C(C=C1C(C)C)C(C)=CC1=O	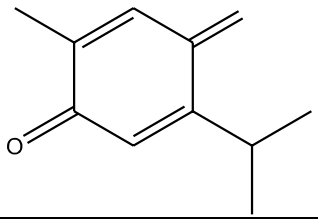
13	2-Cyclohexen-1-one, 2-(2-methyl-2-propenyl)-	O=C1C(CC(C)=C)=CCCC1	

			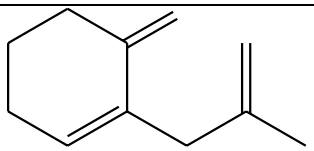
14	Tenovin-6	CN(CCCCC(NC1=CC=C(NC(NC(C2=CC=C(C(C)(C)C)C=C2)=O)=S)C=C1)=O)C	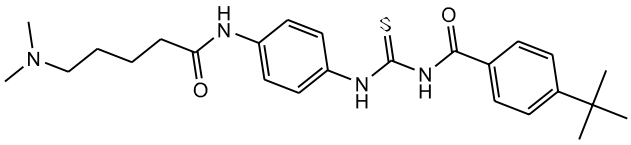
15	Thymol	CC1=CC(O)=C(C(C)C)C=C1	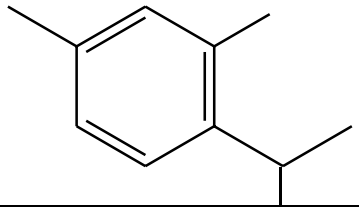
16	3-ethyl-5-isopropyl-2-methyl phenol	OC1=CC(C(C)C)=CC(CC)=C1C	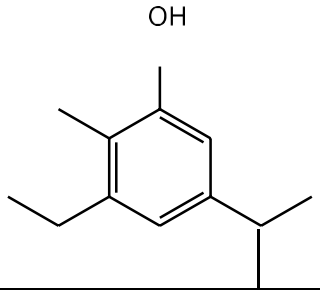
17	2-Methyl-5-(propan-2-ylidene)cyclohexane-1,4-diol	OC1C(C)CC(O)/C(C1)=C(C)/C	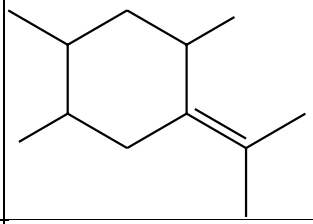
18	2,6-Octadien-1-ol, 3,7-dimethyl-, acetate	C/C(C)=C\CCC(C)=CCOC(C)=O	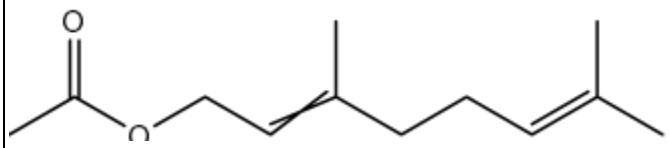
19	p-Cymene-2,5-diol	CC1=CC(O)=C(C(C)C)C=C1O	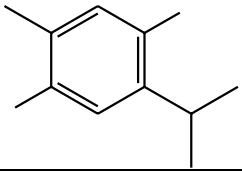
20	2,4-Di-tert-butylphenol	OC1=CC=C(C(C)(C)C)C=C1C(C)(C)C	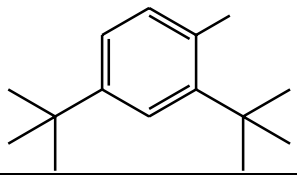
21	2-Tridecenal, (E)-	CCCCCCCCCC/C=C/C=O	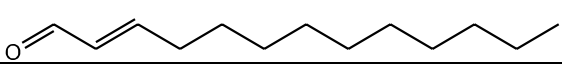

22	Tetradecanoic acid	CCCCCCCCCCCCC(O)=O	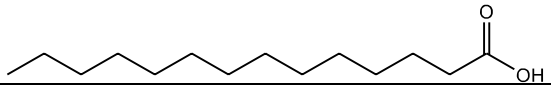
23	Naphthalene, 1,2,3,4,4a,5,6,7-octahydro-4a-methyl-	CC12CCCCC1=CCCC2	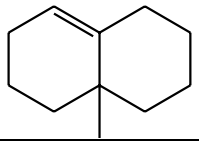
24	Hexadecanoic acid, methyl ester	CCCCCCCCCCCCCCCC(OC)=O	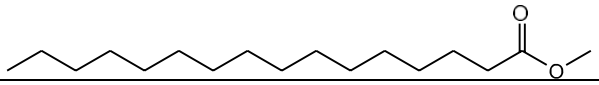
25	n-Hexadecanoic acid	CCCCCCCCCCCCCCCC(O)=O	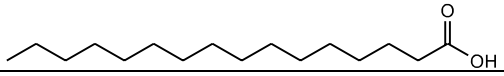
26	Hexadecanoic acid, ethyl ester	CCCCCCCCCCCCCCCC(OCC)=O	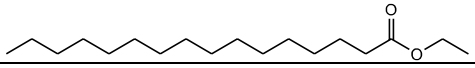
27	9,12-Octadecadienoic acid (Z,Z)-, methyl ester	CCCCC/C=C\C/C=C\CCCCCCCC(OC)=O	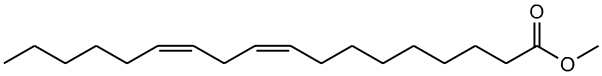
28	6-Octadecenoic acid, methyl ester, (Z)-	CCCCCCCCCCCC/C=C\CCCCC(OC)=O	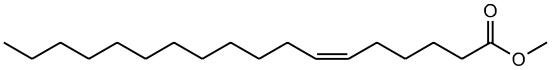
29	9,12-Octadecadienoic acid (Z,Z)-	CCCCC/C=C\C/C=C\CCCCCCCC(O)=O	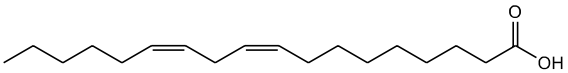
30	9-Octadecenoic acid, (E)-	CCCCCCCC/C=C/CCCCCCCC(O)=O	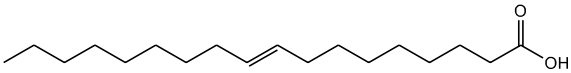
31	Linoleic acid ethyl ester	CCCCC/C=C\C/C=C\CCCCCCCC(OCC)=O	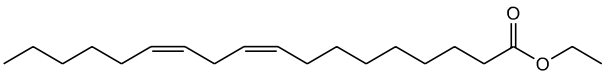
32	Ethyl Oleate	CCCCCCCC/C=C\CCCCCCCC(OCC)=O	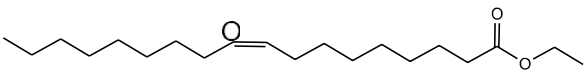
33	Butanedioic acid, 3-hydroxy-2,2-dimethyl-, diethylester	O=C(OCC)C(C)(C)C(O)C(OCC)=O	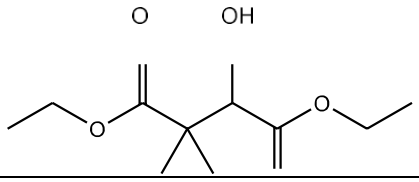
34	Octadecanoic acid, 17-methyl-, methyl ester	CC(C)CCCCCCCCCCCCCCCC(OC)=O	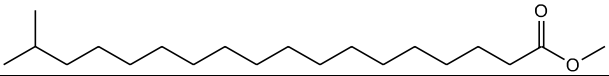

35	Methyl glycocholate, 3TMS derivative	O[C@]1(C[Si](C)(C)C)CC[C@]2(C)[C@@]3([H])C[C@H](O)[C@]4(C)[C@@H]([C@H](C)CCC(NCC([O-])=O)=O)CC[C@@]4([H])[C@]3([H])[C@H](O)CC2C1	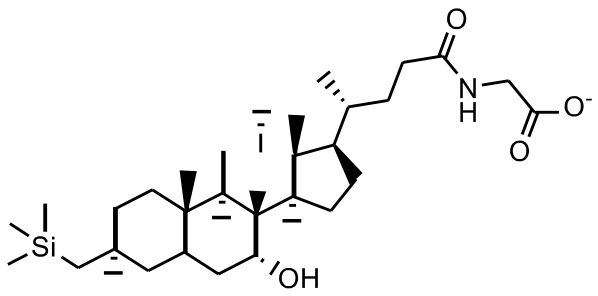
36	Oxiraneoctanoic acid, 3-octyl-, cis-	O=C(O)CCCCCCC[C@H]1O[C@H]1CCCCCCCC	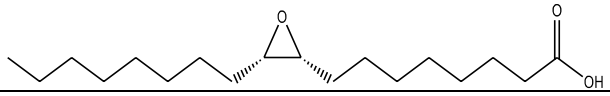
37	Tricyclo[20.8.0.0(7,16)]triacontane, 1(22),7(16)-diepoxy-	C12(O3)CCCCCC4(O5)CCCCCCCCC45CCCCCC13CCCCCCC2	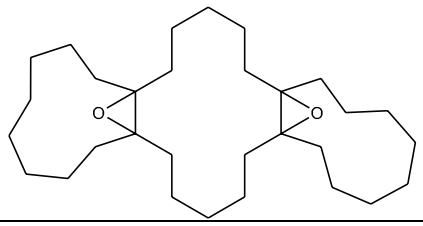
38	Glycidyl oleate	CCCCCCCC/C=C\CCCCCCCC(OCC1CO1)=O	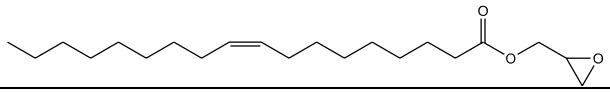

Figure 3 Zone of Inhibition by *C. sativum* on plates spreaded with *S. aureus* [Negative - N control, Positive - P control, T1 10 µL, T2 30 µL , T3 50 µL shows 10, 13, 11, 12, 13 mm respectively]

Table 4 Docking scores of 38 ligands with four proteins using Autodoc vina

S.No.	Active components from C.sativum	Docking score (Kcal / mol) of PDB IDs			
		4F6X	3ACX	2ZCQ	2ZCS
1	Cyclopentanone, 2-methyl-	-3.8	-4.2	-4.5	-4.5
2	(2-Mercaptoethyl)guanidine	-4.5	-4.6	-4.3	-4.4
3	1,2-Diethylhydrazine	-3.3	-3.2	-3.1	-3.3

4	Benzene, 1-methyl-3-(1-methylethyl)-	-4.6	-4.7	-4.5	-4.6
5	ç-Terpinene	-6.4	-6.3	-6.2	-6.4
6	Propane, 1,1,3-triethoxy-	-6.5	-6.5	-6.6	-6.4
7	Linalool	-6.4	-6.4	-6.5	-6.4
8	Bicyclo[3.1.0]hexan-2-ol, 2-methyl-5-(1-methylethyl)-, (1à,2à,5à)-	-6.8	-6.8	-6.8	-6.8
9	Terpinen-4-ol	-6	-6.3	-6.7	-6.8
10	Terpineol	-6.8	-6.6	-6.7	-6.8
11	Bicyclo[3.1.0]hexan-2-ol, 2-methyl-5-(1-methylethyl)-, (1à,2à,5à)-	-6.6	-6.5	-6.6	-6.7
12	Thymoquinone	-6.7	-6.3	-6.7	-6.7
13	2-Cyclohexen-1-one, 2-(2-methyl-2-propenyl)-	-6.5	-6.5	-6.6	-6.5
14	Tenovin-6	-6.9	-6.9	-7.0	-6.9
15	Thymol	-6.4	-6.5	-6.4	-6.6
16	**3-ethyl-5-isopropyl-2-methyl phenol**	**-7.3**	**-7.7**	**-7.7**	**-7.4**
17	2-Methyl-5-(propan-2-ylidene)cyclohexane-1,4-diol	-6.5	-6.4	-6.3	-6.5
18	2,6-Octadien-1-ol, 3,7-dimethyl-, acetate	-6.6	-6.4	-6.6	-6.6
19	p-Cymene-2,5-diol	-6.0	-6.2	-6.3	-6.2
20	**2,4-Di-tert-butylphenol**	**-7.9**	**-7.3**	**-7.3**	**-7.5**
21	2-Tridecenal, (E)-	-7.0	-6.0	-6.2	-6.1
22	Tetradecanoic acid	-6.5	-6.3	-6.3	-6.4
23	Naphthalene, 1,2,3,4,4a,5,6,7-octahydro-4a-methyl-	-6.3	-6.3	-6.4	-6.6
24	Hexadecanoic acid, methyl ester	-6.6	-6.7	-6.6	-6.8
25	n-Hexadecanoic acid	-7.0	-6.8	-6.9	-6.9
26	Hexadecanoic acid, ethyl ester	-6.3	-6.4	-6.4	-6.4
27	9,12-Octadecadienoic acid (Z,Z)-, methyl ester	-6.3	-6.8	-6.3	-6.2
28	6-Octadecenoic acid, methyl ester, (Z)-	-6.6	-6.5	-6.6	-6.5
29	9,12-Octadecadienoic acid (Z,Z)-	-6.2	-6.2	-6.2	-6.2
30	9-Octadecenoic acid, (E)-	-6.3	-6.5	-6.4	-6.6
31	Linoleic acid ethyl ester	-6.7	-6.5	-6.4	-6.6
32	Ethyl Oleate	-6.5	-6.4	-6.4	-6.7
33	Butanedioic acid, 3-hydroxy-2,2-dimethyl-, diethylester	-6.0	-6.0	-6.2	-6.1

34	Octadecanoic acid, 17-methyl-, methyl ester	-6.5	-6.3	-6.3	-6.4
35	Methyl glycocholate, 3TMS derivative	-6.3	-6.3	-6.4	-6.6
36	Oxiraneoctanoic acid, 3-octyl-, cis-	-6.6	-6.7	-6.6	-6.8
37	Tricyclo[20.8.0.0(7,16)]triacontane, 1(22),7(16)-diepoxy-	-6.0	-6.8	-6.9	-6.9
38	Glycidyl oleate	-6.3	-6.4	-6.4	-6.4

Fig 4a 3D & 2D diagram of ligand 1 with 4F6X

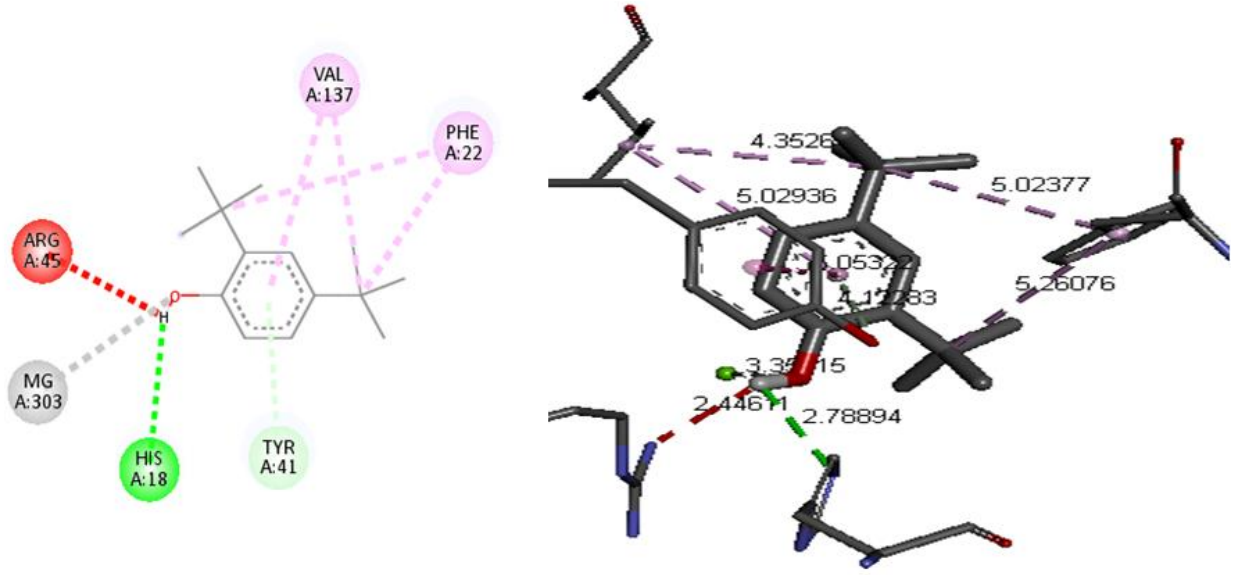

Fig 4b 3D & 2D diagram of ligand 2 with 3ACX

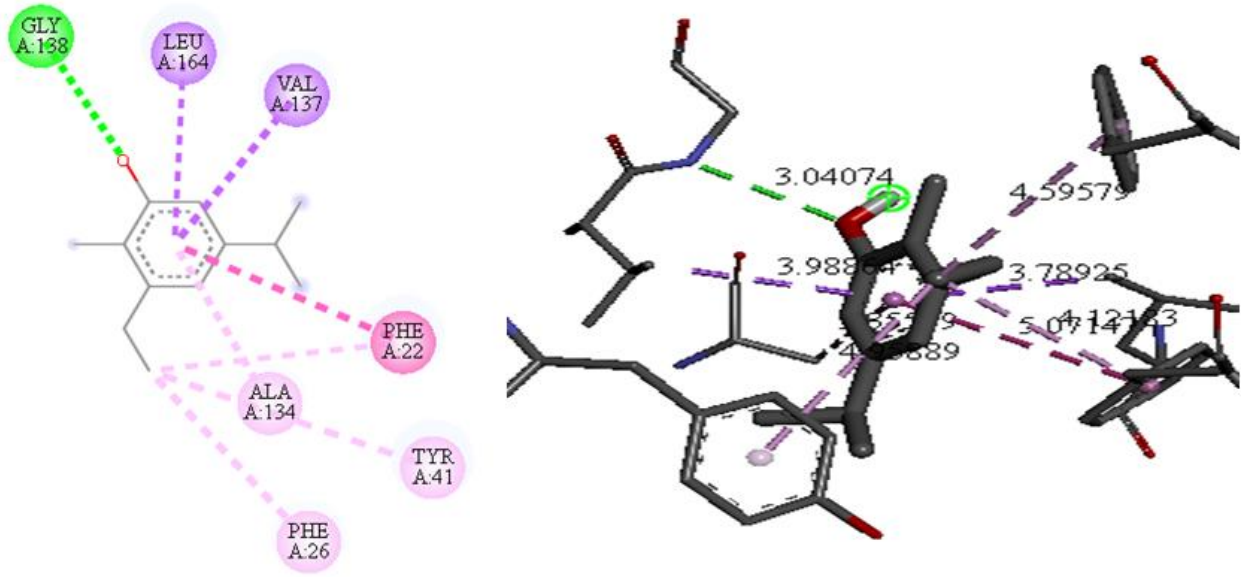

Fig 5a 3D & 2D diagram of ligand 2 with 2ZCS

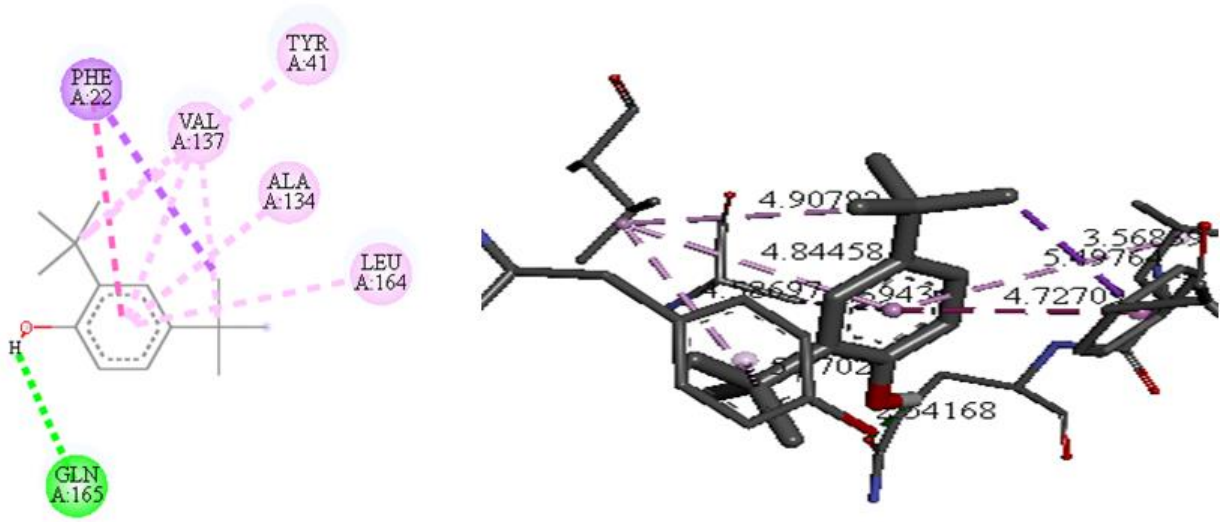

Fig 5b 3D & 2D diagram of ligand 1 with 2ZCQ

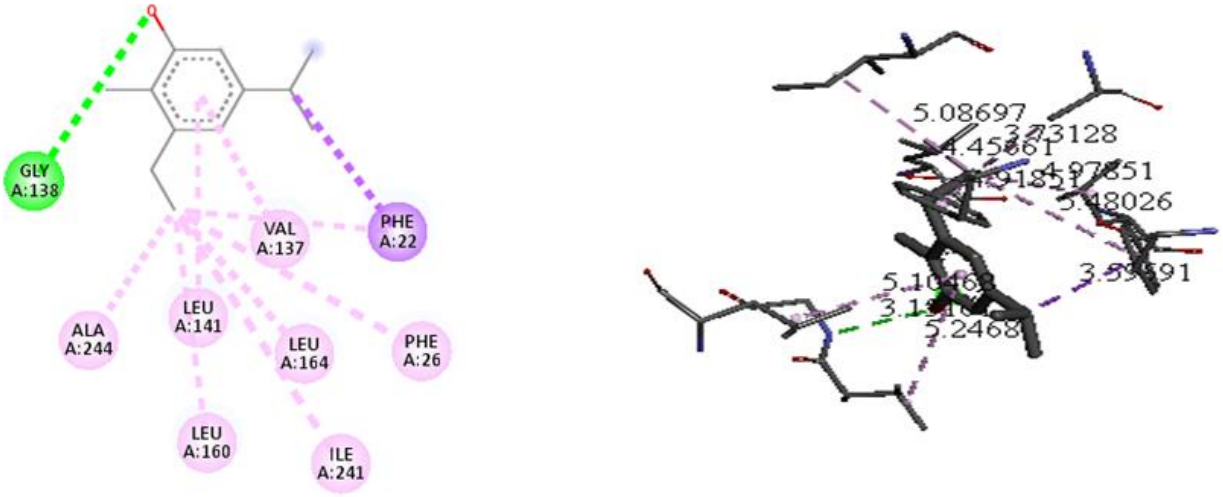

Table 5 Molecular dockings executed using the AutoDock, vina tools

Protein ID	Ligand name	Docking score (kcal / mol)	Type of interaction Donor: Acceptor	Distance (Å)	Bonding Type
4f6x	2,4-di-tert-butylphenol	-7.9	HIS18 (N-H…O)	2.78894	H Bond
3acx	3-ethyl-5-isopropyl-2-methylphenol	-7.7	GLY138 (N-H…O)	3.04074	H Bond
			ASN168 (O…H-N)	2.38693	
			ASN168 (O…H-N)	2.67893	
			ARG45 (N-H…N)	3.08172	
			TYR41 (N-H…O)	2.77676	
2zcq	3-ethyl-5-isopropyl-2-methylphenol	-7.7	GLY138 (N-H…O)	3.15161	H Bond
			GLY161 (N-H…O)	2.30173	
2zcs	2,4-di-tert-butylphenol	-7.5	GLN165 (N-H…N)	2.54168	H Bond
			ASP49 (O…H-N)	2.37942	
			ASN168 (O…H-N)	2.41426	
			TYR41 (N-H…O)	3.02218	

Table 6 ADMET, Pharmacokinetics and Drug likeliness properties of ligands

Property	Model name	2, 4-di-tert-butyl phenol	3-ethyl-5-isopropyl-2-methyl phenol
Lipinski's rule of five	Molecular weight	206.32 g/ mol	178.27 g/mol
	HBD (should be <5)	1	1
	HBA (should be <10)	1	1
	TPSA	20.23 Å²	20.23 Å²
	log P (should be <5)	3.99	3.39
Absorption	Water solubility	-2.337 log mol/L	-2.518 log mol/L
	Caco2 permeability	0.8168 log Papp in 10^{-6} cm/s	0.8560 log Papp in 10^{-6} cm/s
	Intestinal absorption (human)	99.52 % Absorbed	99.66 % Absorbed
	Skin Permeability	-4.68 log Kp	-4.65 log Kp

	P-glycoprotein substrate	No	No
	P-glycoprotein I inhibitor	No	No
	P-glycoprotein II inhibitor	No	No
Distribution	VDss (human)	-0.314 log L/kg	-0.138 log L/kg
	Fraction unbound (human)	0.155 Fu	0.155 Fu
	BBB permeability	Yes	Yes
	CNS permeability	-2.478 log PS	-2.574 log PS
Metabolism	CYP1A2	No	No
	CYP2C19	No	Yes
	CYP2C9	Yes	No
	CYP2D6	No	No
	CYP3A4	No	No
	CYP2E1	No	No
Excretion	Renal OCT2 substrate	No	No
Toxicity	Mitochondrial Membrane Potential (MMP)	Yes	Yes
	Ecotoxicity	Yes	Yes
	BBB-barrier	Yes	Yes
	Hepatotoxicity	Yes	No
	Skin Sensitisation	Yes	Yes
	Acute oral toxicity	1.914 Log(1/(mol/kg)	2.484 Log(1/(mol/kg)
	Oral Rat Acute Toxicity (LD50)	700 mg / kg	1030 mg / kg
	Tetrahymena pyriformis	1.866 pIGCO50 ug/l	1.163 pIGCO50 ug/l

Fig 6a-1, 6a-2 The Hydrogen Bond PDB ID: 4F6X, 3ACX during 100 ns simulation using Gromacs software

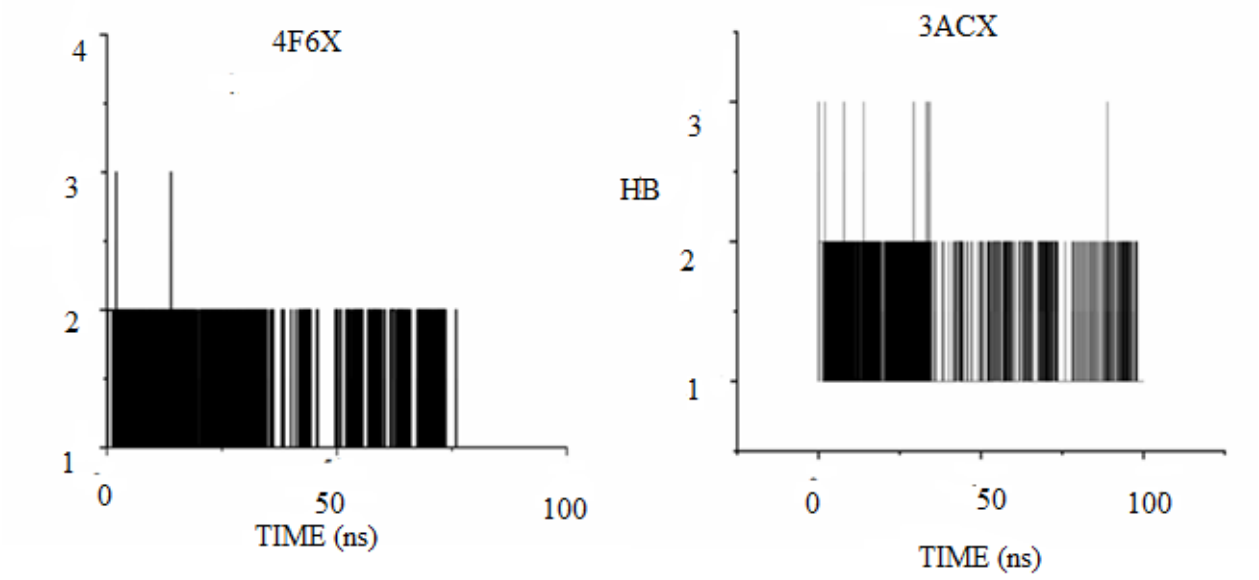

Fig 6b-1, 6b-2 The Hydrogen Bond PDB ID: 2ZCQ, 2ZCS during 100 ns simulation using Gromacs software

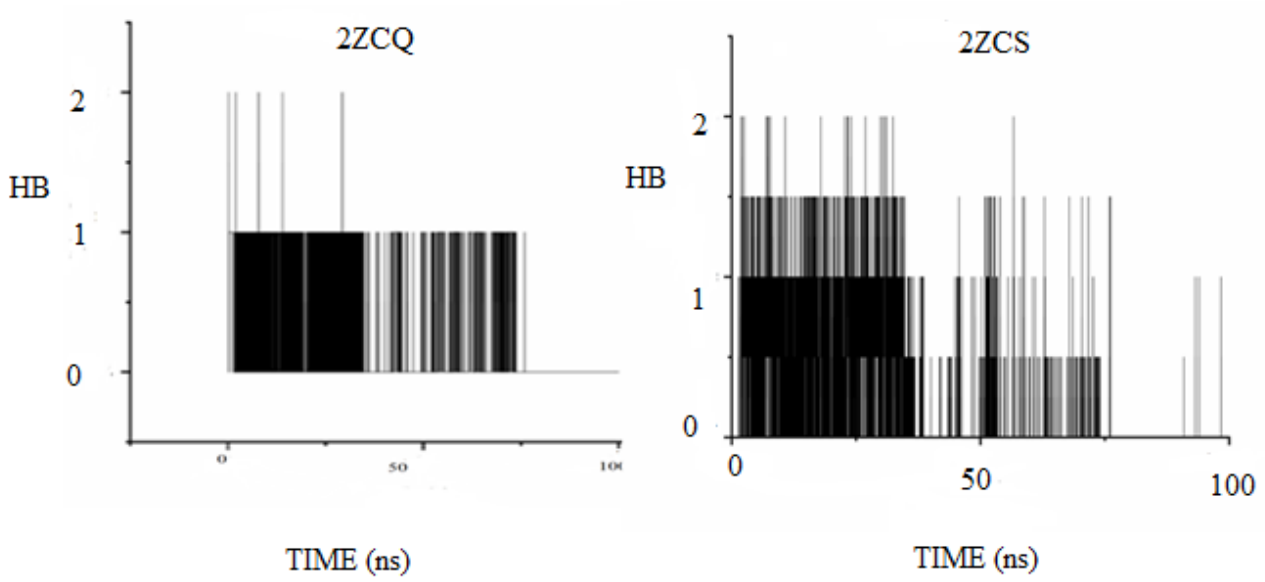

Fig 7a-1, 7a-2 The protein - ligand RMSD plots of the ligand in complex with the proteins PDB ID: 4F6X, 3ACX during 100 ns simulation using Gromacs software

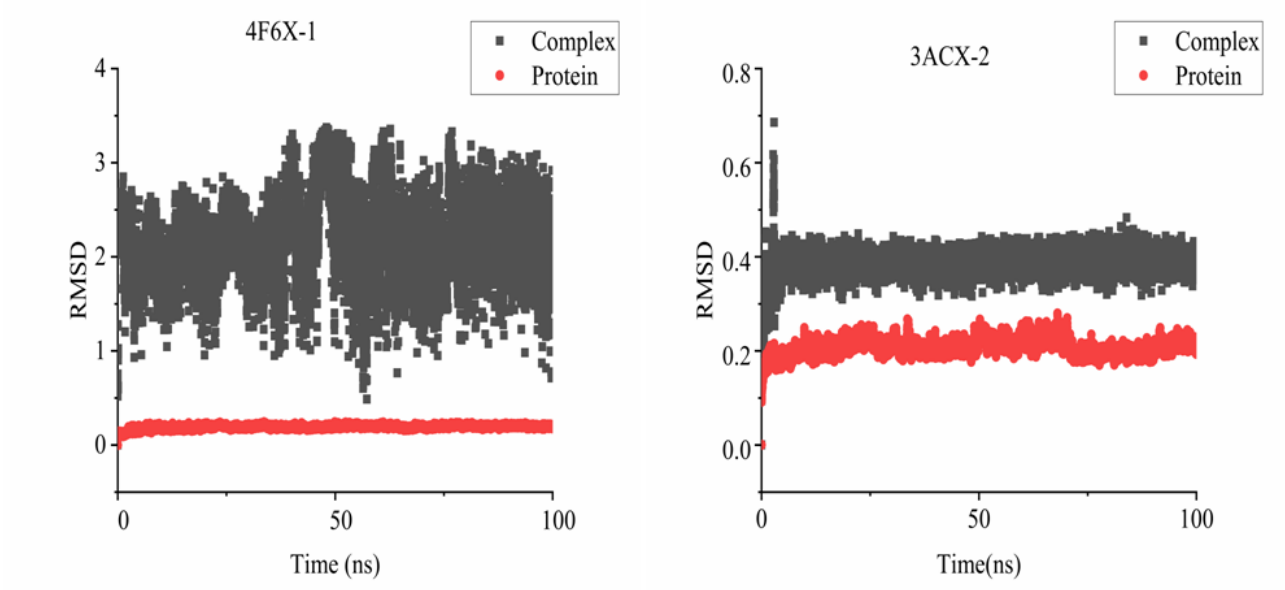

Fig 7b-1, 7b-2 The protein – ligand RMSD plots of ligand in complex with the proteins, PDB ID:2ZCQ, 2ZCS during 100ns simulation using Gromacs software

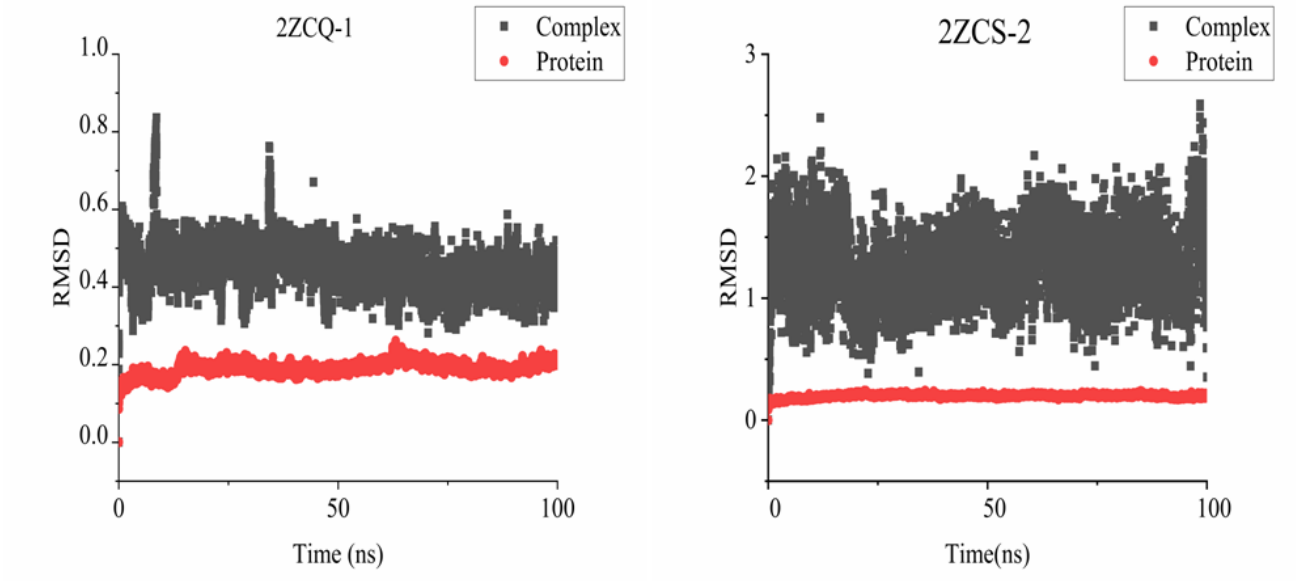

Fig 8a-1, 8a-2 The protein RMSF of PDB ID: 4F6X, 3ACX in complex with the ligand during 100 ns using Gromacs software

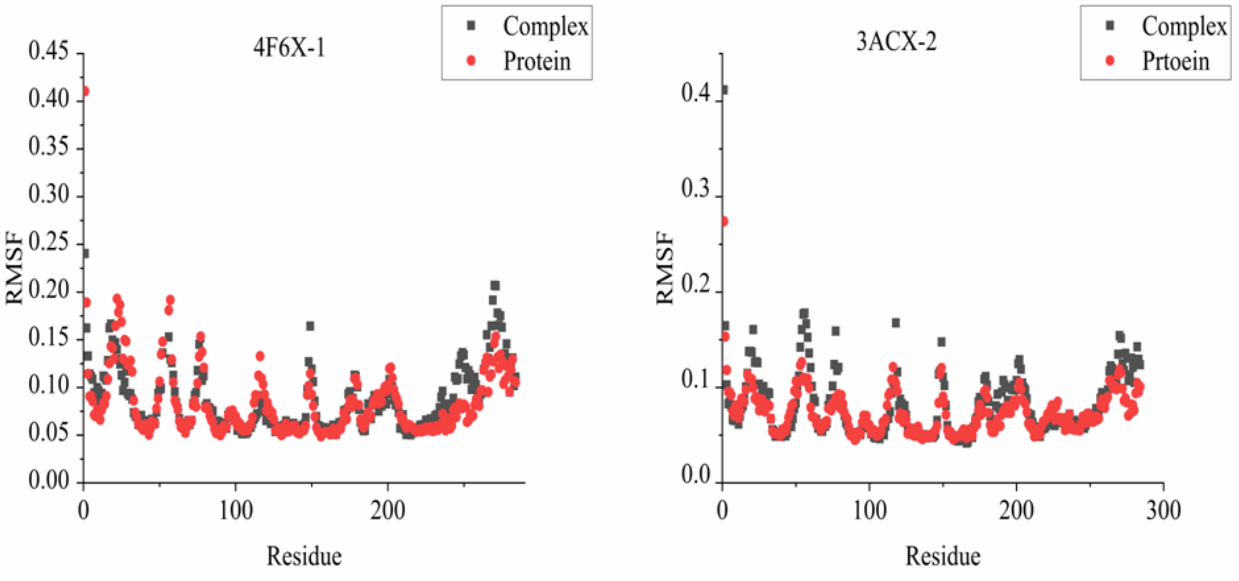

Fig 8b-1, b-2 The protein RMSF of PDB ID: 2ZCQ, 2ZCS in complex with the ligand during 100 ns using Gromacs software

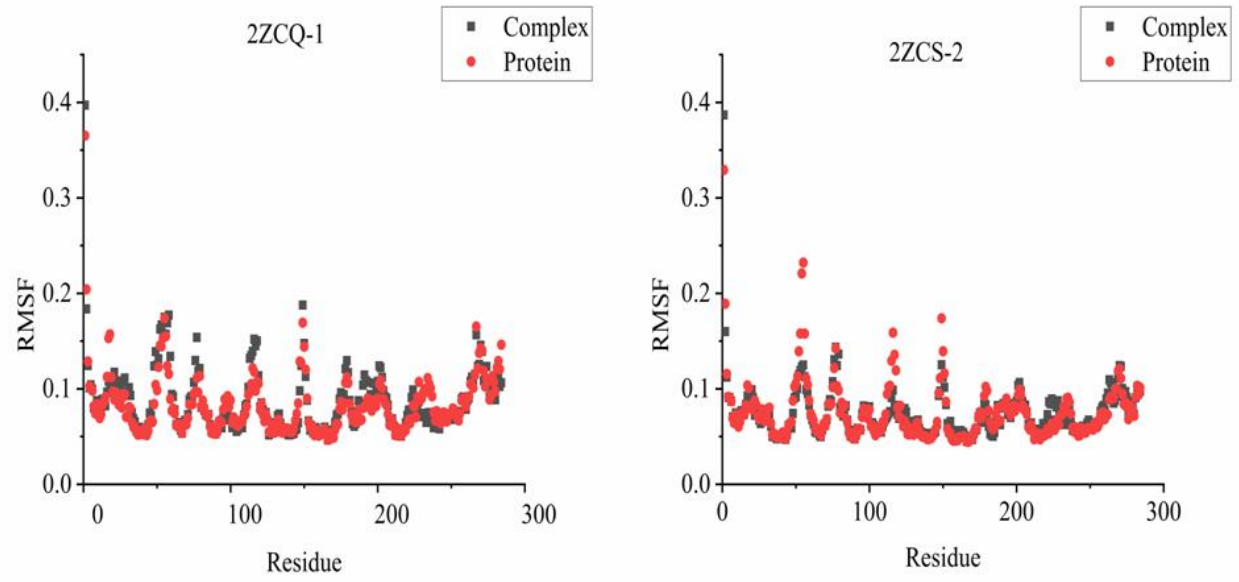

Fig 9a-1, 9a-2 The Radius of gyration plots of the ligand in complex with the proteins PDB ID: 4F6X, 3ACX during 100 ns simulation using Gromacs software

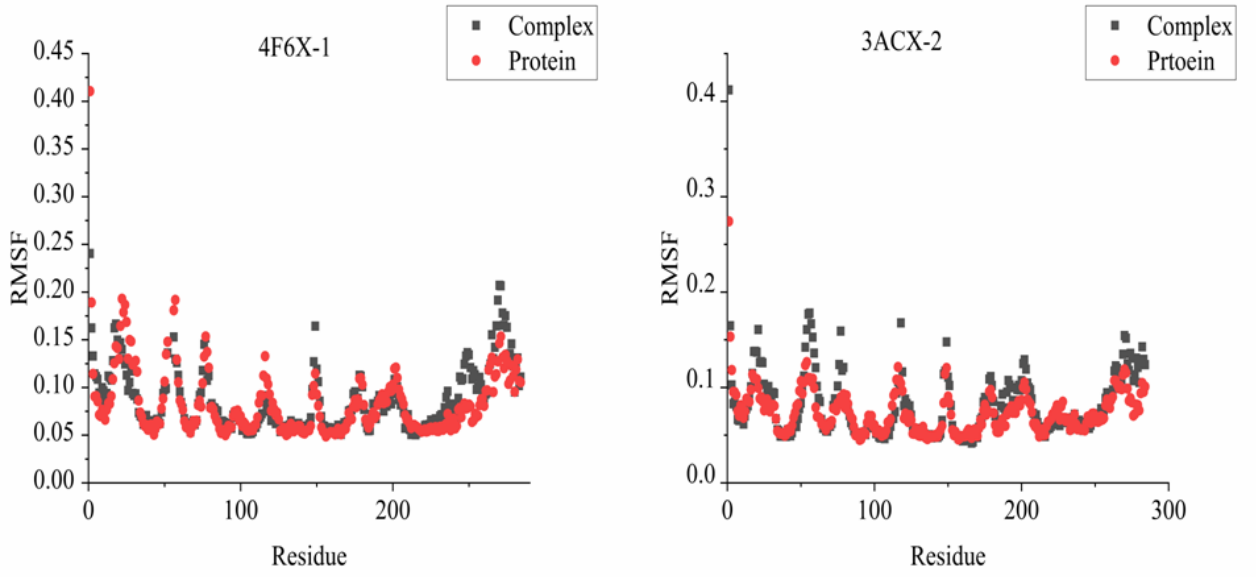

Fig 9b-1, 9b-2 The Radius of gyration plots of the ligand in complex with the proteins PDB ID: 2ZCQ, 2ZCS during 100 ns simulation using Gromacs software

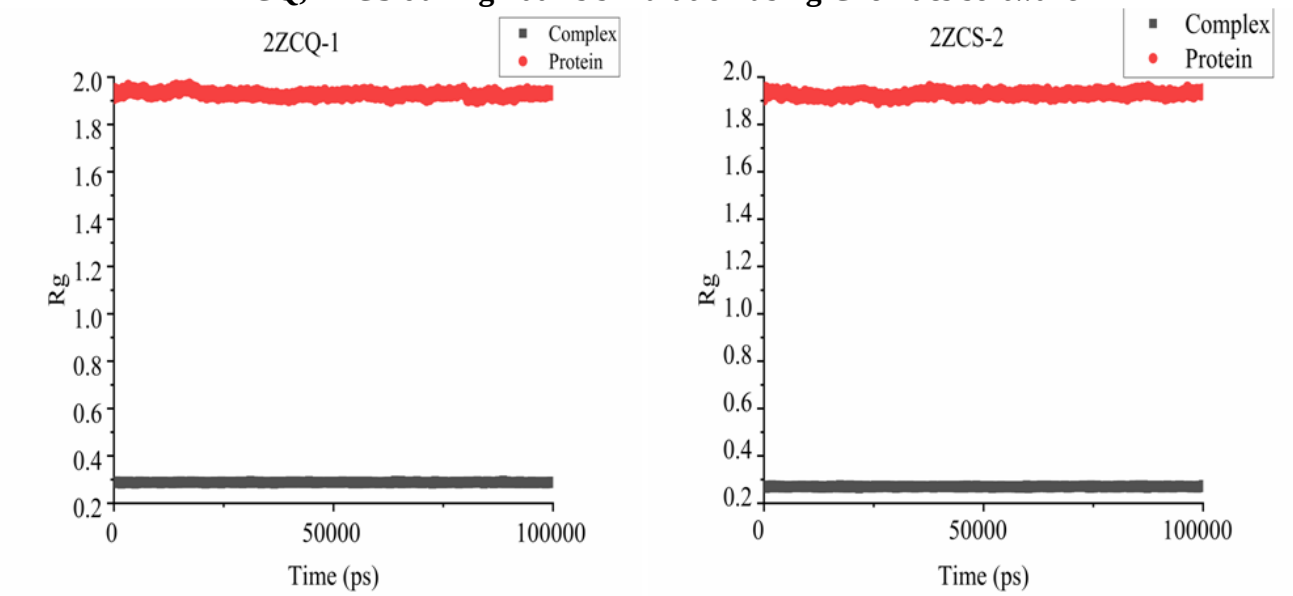

Fig 10a-1, 10a-2 The ligand – protein, PDB ID: 4F6X, 3ACX plot shows SASA using Gromacs software

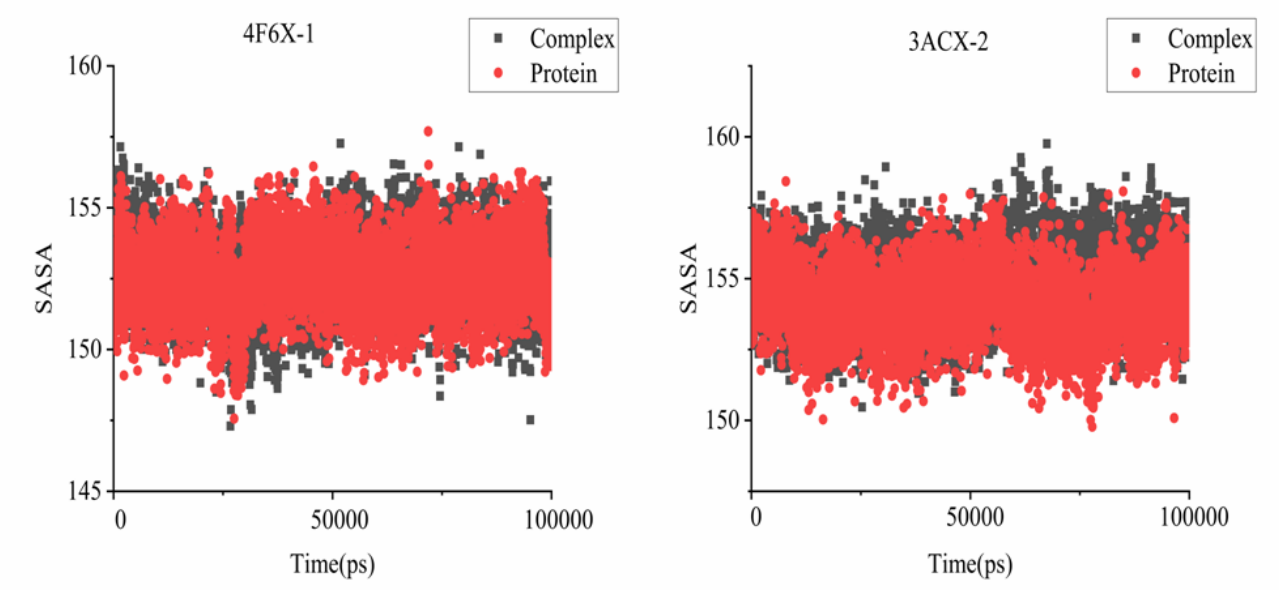

Fig 10b-1, 10b-2 The ligand – protein, PDB ID: 2ZCQ, 2ZCS plot shows SASA using Gromacs software

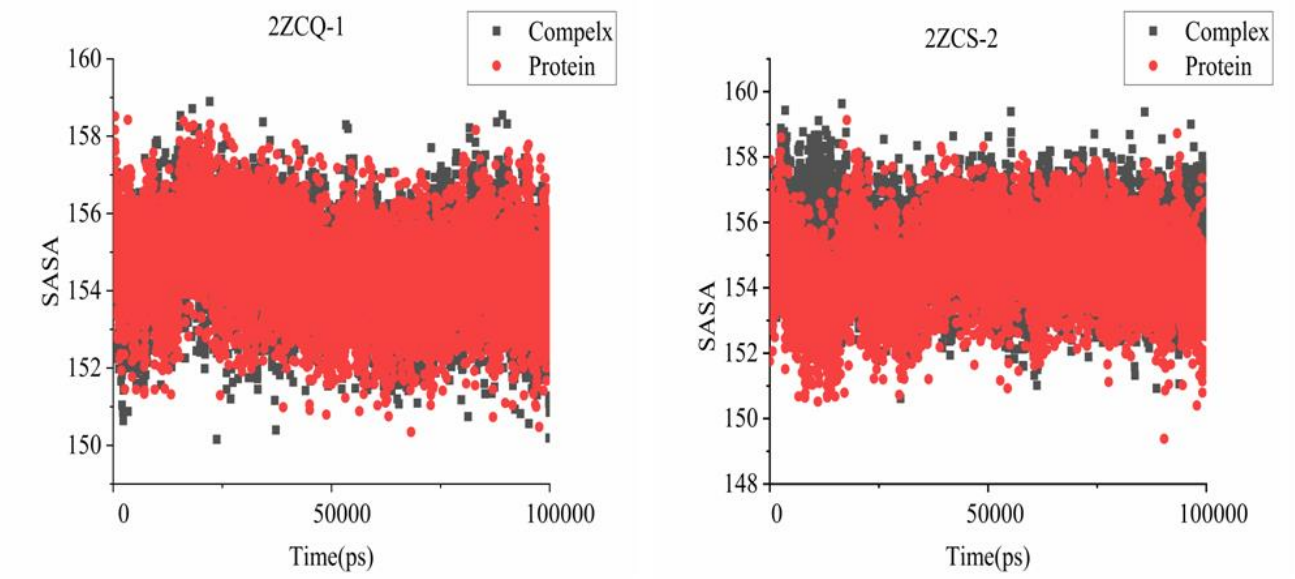

Fig 11a-1, 11a-2 The ligand – protein, PDB ID: 4F6X, 3ACX plot shows Radial Distribution Function g(r) using Gromacs software

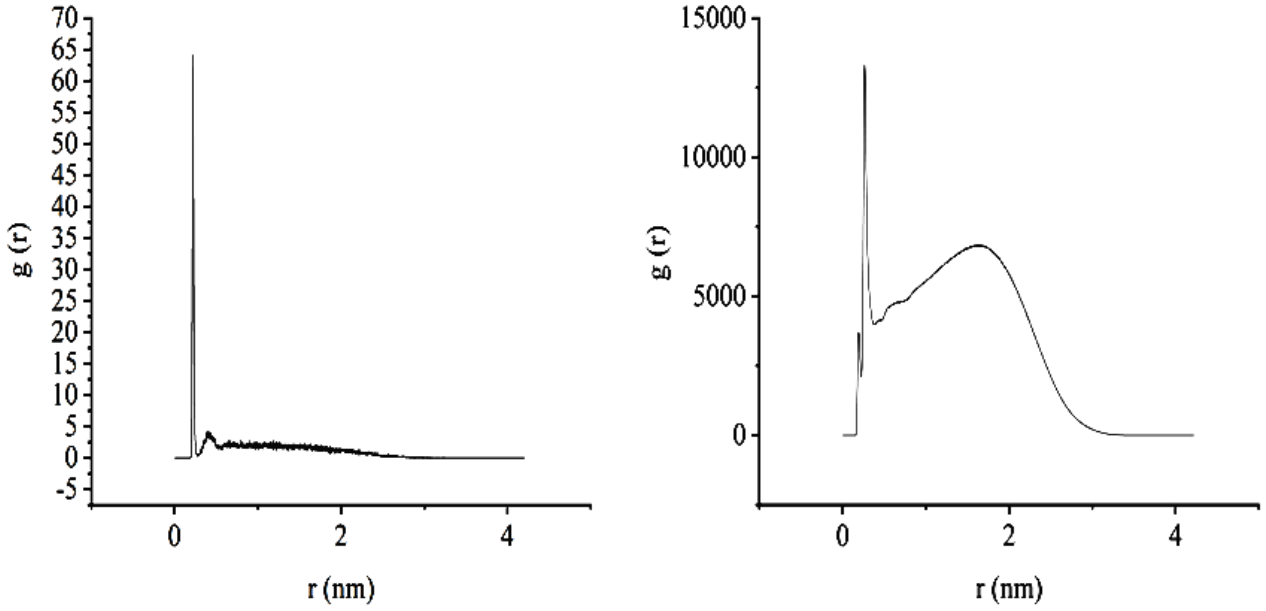

Fig 12a-1, 12a-2 The ligand – protein, PDB ID: 2ZCQ, 2ZCS plot shows Radial Distribution Function g(r) using Gromacs software

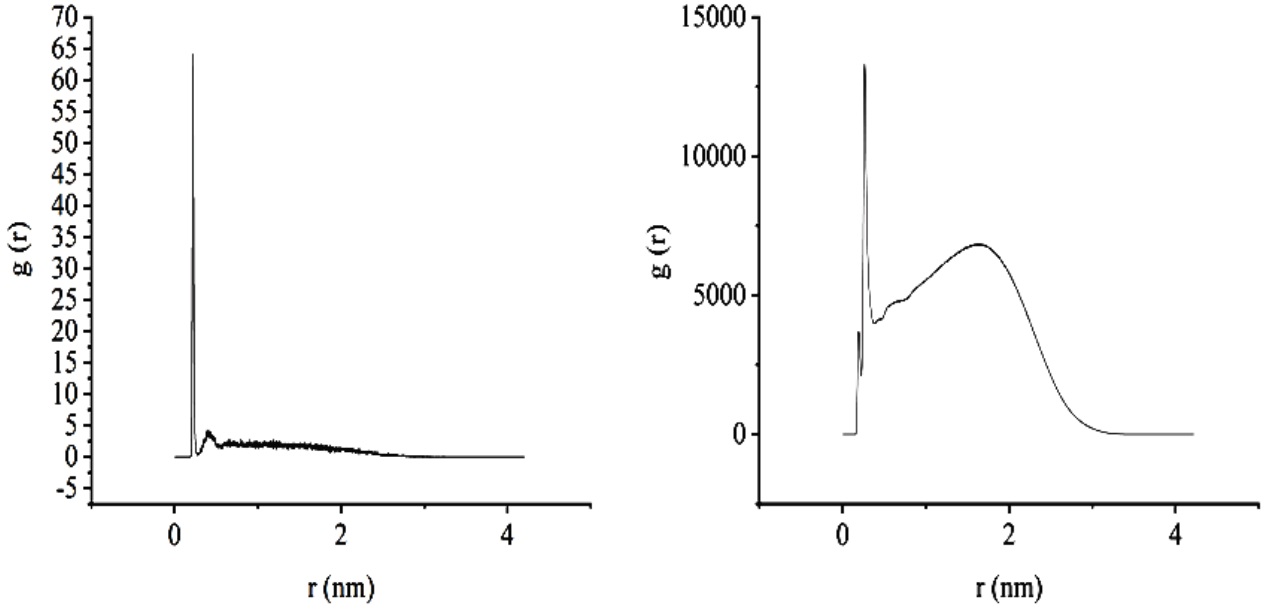

Table 7 Interaction energy of the different protein with ligands (values in kCal/mol)

Unit (kCal / mol)	4F6X with ligand 1	3ACX with ligand 2	2ZCQ with ligand 2	2ZCS with ligand 1
ΔEVDW (van der Waal energy)	37.18	-25.62	34	-27.39
ΔEElectro (Electrostatic energy)	-2420.83	1.4	-1839	-9.91
Non polar solvation energy (SASA energy)	0	-3.78	0	-3.9
ΔGsolv (Polar Solvation energy)	2390.63	11.06	1785.29	19.12
ΔGnp (Non polar solvation free energy)	-2383.65	-24.23	-1805	-37.3
ΔGpolar (Polar solvationfree energy)	2390.63	7.28	1785.29	15.22
ΔS (Entropy)	84.15	2.23	38.88	2.87
ΔGbind (Total BindingEnergy)	192.27	-14.02	99.46	-16.1

Biographies

Sharmil Suganya R is Assistant Professor in Government College of Engineering, Salem, Tamil Nadu, received B.Tech degree in Biotechnology from Bharathidasan University, Trichy, Tamil Nadu, M.Sc. degree in Biomedical Instrumentation Science from Madras University, Chennai and M.S. (By Research) degree in Biotechnology from Anna University, Chennai in the years 2004, 2006 and 2020 respectively. Her research interest is in Biotechnology, Microbial corrosion, and drug delivery system.

Sugan S received B.Sc. & M.Sc. degrees in Chemistry from Periyar University Salem and B.Ed. degree in Tamil Nadu Teacher's Education Board, Chennai in the years 2017, 2019 and 2021 respectively. His research interest is in Organic Chemistry, Medicinal Chemistry and drug delivery system.

Venugopal T is Assistant Professor in the Department of Chemistry, Government College of Engineering, Salem, Tamil Nadu, received B.Sc. & M.Sc. degrees in Chemistry from Madras University, M.Phil degree in Chemistry from Bharathidasan Universtiy, Trichy and Ph.D in Chemistry Madras University, Chennnai in the years 1993, 1995, 2004 and 2009 respectively. His research interest is in Phytochemistry, Corrosion, Organic Chemistry, Bioinformatics, Cheminformatics, Nanoscience and Nanotechnology, Nanocomposite polymers and drug delivery system.